GEOPHYSICS, VOL. 82, NO. 3 (MAY-JUNE 2017); P. C91–C111, 6 FIGS., 3 TABLES.
10.1190/GEO2015-0621.1

Fourth-order normal moveout velocity in elastic layered orthorhombic media — Part 1: Slowness-azimuth domain

Igor Ravve[1] and Zvi Koren[1]

ABSTRACT

Considering all types of pure-mode and converted waves, we derive the azimuthally dependent, fourth-order normal moveout (NMO) velocity functions, and hence the corresponding effective anellipticity functions, for horizontally layered orthorhombic media. We emphasize that this paper does not suggest a new nonhyperbolic traveltime approximation; rather, it provides exact expressions of the NMO series coefficients, computed for normal-incidence rays, which can then be further used within known azimuthally dependent traveltime approximations for short to moderate offsets. We do not assume weak anisotropy or acoustic approximation for P-waves. At each layer, the elastic parameters, thickness, and azimuth of the orthorhombic vertical symmetry planes are considered to be different. We distinguish between two different azimuths: slowness azimuth (part 1 of this paper) and offset azimuth (part 2 of this paper). In part 1, the slowness-azimuth domain NMO is approximated as a series of either infinitesimal horizontal slowness (slowness-azimuth/slowness domain) or infinitesimal offsets (slowness-azimuth/offset domain). Similarly, in part 2, we distinguish between two offset-azimuth domains: offset-azimuth/slowness and offset-azimuth/offset. Note that the azimuthally dependent NMO velocity functions of each of the four cases are different. The validity of the method is tested by introducing our derived azimuthally dependent, fourth-order effective anellipticity, into the well-known azimuthally dependent, asymptotic nonhyperbolic traveltime approximation, in which we compare the traveltime approximation versus exact numerical ray tracing for short to moderate offsets. It is clearly shown that for these types of azimuthally anisotropic layered models, the fourth-order terms are essential even for relatively small horizontal-slowness values or short offsets.

INTRODUCTION

Orthorhombic models comprise subsurface anisotropy caused by vertical, azimuthally aligned stress/fractures and fine layering or that caused by two different orthogonal sets of vertical, azimuthally aligned stress/fractures, with or without fine layering. This work focuses on the forward computation of local (single layer) and then global (multilayer) effective parameters of layered orthorhombic models and the corresponding second- and fourth-order normal moveout (NMO) velocity functions. Note that the concept of local and global effective parameters for azimuthally isotropic layered media (e.g., Dix, 1955) has been widely used for interval velocity parameter estimation and seismic imaging.

We consider all types of pure-mode and converted waves, in which the layers have a common horizontal symmetry plane but different orientations of the vertical symmetry planes and different orthorhombic parameters. Obviously, some of the layers can be characterized with isotropy, VTI, or HTI realizations, which are parameterized as particular cases of orthorhombic anisotropy.

The forward computation of second-order global NMO velocities in multilayer orthorhombic media as a function of the offset-azimuth ψ_{off} (e.g., Grechka and Tsvankin, 1998, 1999; Bakulin et al., 2000, 2002) and as a function of the slowness azimuth ψ_{slw} (Koren et al., 2013; Ravve and Koren, 2013, 2015a; Koren and Ravve, 2014) has already been intensively studied. It has been shown that the traveltime accuracy obtained using only second-order NMO velocities is not sufficient for analyzing conventional offset-domain seismic reflection events (with half-offset to depth ratio up to one). Fourth-order terms are essential. Nonhyperbolic reflection moveout in a layered HTI medium is studied in the offset-azimuth domain by Al-Dajani and Tsvankin (1998) and in the slowness-azimuth domain by Ravve and Koren (2010) and Koren et al. (2010). For a single-layer ortho-

Manuscript received by the Editor 11 November 2015; revised manuscript received 5 December 2016; published online 13 March 2017.
[1]Paradigm Geophysical, R and D, Houston, Texas, USA. E-mail: igor.ravve@pdgm.com; zvi.koren@pdgm.com.

rhombic model whose reflection surface coincides with the horizontal plane of symmetry, the offset-azimuth domain fourth-order NMO velocity is derived by Al-Dajani et al. (1998) and Al-Dajani and Toksoz (2001) (for any strength of anisotropy), and for a dipping single-layer model by Pech and Tsvankin (2004) (for weak anisotropy and for fracture azimuth coinciding with the dip azimuth). Pech et al. (2003) proposed an explicit formula of the quartic coefficient for compressional waves in general anisotropic layers and applied it to a single tilted transverse isotropy (TTI) layer. Vasconcelos and Tsvankin (2006) implement an azimuthally dependent traveltime approximation to invert orthorhombic layered parameters. Stovas (2015) studies the NMO velocity in a multilayer orthorhombic medium with different azimuths of the orthorhombic vertical symmetry planes and derives acoustic approximate expressions for effective anellipticity in the slowness-azimuth and offset-azimuth domains. In the cited work, the effective anellipticity is based on three parameters: $\eta_1, \eta_2, \eta_{xy}$ in the slowness-azimuth domain and N_1, N_2, N_{xy} in the offset-azimuth domain. Additionally, several acoustic approximations of the phase and ray velocities in orthorhombic media have recently been proposed (Sripanich and Fomel, 2014; Hao and Stovas, 2015, 2016), which are accurate for a wide range of reflection angles. Sripanich and Fomel (2016) propose an extension formula of fourth-order NMO velocity for general anisotropy, which was used for estimating local (interval) parameters of layered orthorhombic models with rotated azimuths. Ivanov and Stovas (2016) study the influence of shear wave singularities on the NMO velocity ellipse in tilted orthorhombic media.

We recently derived the exact fourth-order effective velocity as a function of the slowness azimuth for quasi-P-waves in horizontally layered orthorhombic media, and we briefly presented the theory in the extended abstracts (Koren and Ravve, 2015, 2016; Ravve and Koren, 2015b, 2016). The primary objective of this study is to provide a full derivation of the results presented in these abstracts. Moreover, in part 1 of this paper, we extend the theory to all types of waves, and in part 2, we derive the second-order relation for the lag between the offset azimuth and slowness azimuth, which makes it possible to obtain the fourth-order offset-azimuth domain NMO velocity as well. The azimuthally dependent global fourth-order NMO velocity $V_4(\psi)$, along with the quartic moveout coefficient $A_4(\psi)$ and effective anellipticity $\eta_{\text{eff}}(\psi)$, are exact functions of the slowness or offset azimuth. The exact functions, however, require five (rather than three) fourth-order coefficients (in addition to the well-known three second-order coefficients). It is important to note that the resulting eight global effective parameters are associated with lower symmetries (such as monoclinic anisotropy) than those of the individual orthorhombic layers. While the horizontal symmetry plane is still shared by all layers, the change in azimuths of the vertical symmetry planes at each layer ruins the vertical symmetry of the global effective model.

The main objectives for deriving the slowness-azimuth domain fourth-order NMO velocity function are the following: First, it is the primary step required for obtaining the offset-azimuth domain fourth-order NMO velocity function (presented in part 2 of this paper). The new aspects of this work are that we do not make any assumption of weak anisotropy or acoustic approximation for P-waves and that our derived fourth-order coefficients are valid for all types of pure-mode and converted waves. Second, the slowness azimuth and offset azimuth, second- and fourth-order NMO velocities can be used for updating the background interval parameters of orthorhombic layered models when using residual moveouts (RMOs) analyzed along migrated common image gathers (CIGs). The commonly used CIGs for updating azimuthally varying anisotropic models should obviously include azimuthal information. These gathers are normally classified into two main types of Kirchhoff-based migrations: the conventional offset domain and the reflection (or opening) angle domain (e.g., Koren and Ravve, 2011; Ravve and Koren, 2011), in which the angles refer to the opening angles and azimuths between the two slowness vectors of the incident and reflected waves at the image points (slowness-azimuth domain). This is why the two different azimuthal domains (slowness and offset) are so important.

To obtain the fourth-order NMO velocity functions, we first derive the series for the two offset components and the traveltime for a given slowness azimuth and for small horizontal slowness, referred to as the slowness-azimuth/slowness domain. To compute these series, we first consider a single layer and derive the relations for the Cartesian components of the ray velocity using the vertical-slowness surface function. The latter is obtained by solving the Christoffel equation for the given horizontal-slowness components and the given elastic parameters. Next we compute the contributions of any given layer into the following three propagation components: (1) the radial-offset component (along the slowness azimuth), (2) the transverse-offset component (in its perpendicular direction), and (3) the total traveltime. We then provide explicit expression for the fourth-order NMO velocity function (and hence the global effective anellipticity) in the slowness-azimuth/slowness and the slowness-azimuth/offset domains.

The global second- and fourth-order NMO velocity functions are used in updating the velocity model in two different stages. The first stage includes computation of the vertical time (and hence the average velocity) and eight second- and fourth-order, local and then global effective parameters from the background interval orthorhombic layered models (a forward Dix-type summation approach). The second stage involves updating the computed background global effective parameters from azimuthally varying RMOs analyzed along the CIGs. This RMO analysis requires an explicit RMO expression as a function of the (1) (already known) background global effective parameters and (2) the (unknown) residual second- and fourth-order NMO velocities. The RMO expression is obtained by taking the full differential of the azimuthally dependent fourth-order NMO expression, with respect to the residual global effective parameters. Koren and Ravve (2014) suggest a Dix-type inversion to convert the azimuthally anisotropic, global effective second-order parameters into three local (layer) effective parameters, and finally to obtain updated interval orthorhombic parameters δ_1 and δ_2. The extension of the azimuthally dependent NMO velocity to the fourth-order, presented in this paper, makes it possible to use this Dix-type approach to invert for the five fourth-order local effective parameters (in addition to the three second-order parameters). These second- and fourth-order eight local effective parameters can then be transformed (with some a priori assumptions and constraints) into the full set of Tsvankin's (1997) orthorhombic parameters per layer. The inversion process, however, is beyond the scope of this paper.

The body of this paper describes the main steps of the method; the detailed derivations are moved to a corresponding series of appendices. For clarity, a full list of notations is given at the end of the paper. Finally, we demonstrate the feasibility of the derived expressions with a synthetic multilayer model containing strong orthorhombic parameters, simulating compacted sediment layers af-

fected by aligned tectonic stress that yields vertical fracture planes with a different azimuth at each layer. The validity of the derived formulas is tested by introducing our derived, azimuthally dependent, fourth-order anellipticity parameter into the well-known, azimuthally dependent, asymptotic nonhyperbolic traveltime approximation (e.g., Vasconcelos and Tsvankin, 2006), for short to moderate offsets versus exact numerical ray tracing.

BACKGROUND AND BASIC DEFINITIONS

Before describing the main derivations, we provide a brief background and basic definitions of the principal terms used.

Orthorhombic axes, local and global frames

We define the term "orthorhombic axes" x_i as the intersection lines of the orthorhombic symmetry planes $[x_i x_j]$ and $[x_i x_k]$, where indices i, j, k are all different. Orthorhombic axes constitute the local frame of reference for each layer. The azimuth of the vertical symmetry planes can vary from layer to layer. However, all layers (local frames) share the same horizontal symmetry plane and therefore the same vertical axis, which is also the vertical axis of the global frame (Cartesian system of coordinates).

Slowness azimuth and offset azimuth

The term slowness azimuth ψ_{slw} is related to the azimuth of the slowness vector. It also coincides with the azimuth of the horizontal-slowness vector (because the vertical component has no effect on the azimuth) and the azimuth of the phase velocity. Offset azimuth ψ_{off} refers to the azimuths of the surface acquisition sources and receivers. The slowness azimuth and offset azimuth are measured from the global axis x, positive counterclockwise.

Slowness-azimuth domain

We distinguish between two types of slowness-azimuth domain NMO velocities, related to two different slowness-azimuth domain traveltime functions. The first is related to a traveltime approximation series versus infinitesimal horizontal slowness, and it is called the "slowness-azimuth/slowness" domain. The second is associated with a traveltime approximation series versus infinitesimal offsets, and it is called the slowness-azimuth/offset domain.

Offset-azimuth domain

We distinguish between two types of offset-azimuth domain NMO velocities, related to two different offset-azimuth domain traveltime functions. The first is related to a traveltime approximation series versus infinitesimal horizontal slowness, and it is called the "offset-azimuth/slowness" domain. The second is associated with a traveltime approximation series versus infinitesimal offsets, and it is called the offset-azimuth/offset domain.

Overall, we distinguish between three different types of model parameters: interval, local effective, and global effective.

Interval parameters

Nine elastic and two geometric parameters exist for each layer:

1) elastic parameters
   - vertical compressional velocity (v_P)
   - vertical velocity of S-waves polarized in the x_1-direction (v_{S,x_1})
   - seven normalized orthorhombic parameters introduced by Tsvankin (1997), which are extensions to Thomsen (1986) parameters of transverse isotropy $(\delta_1, \delta_2, \delta_3, \varepsilon_1, \varepsilon_2, \gamma_1, \gamma_2)$
2) geometric parameters
   - thickness of a layer (Δz)
   - azimuthal orientation of an orthorhombic axis (ψ_{x_1}).

Both types of notations namely, the explicit stiffness matrix components and Tsvankin's orthorhombic parameters are used in this paper. We therefore listed their two-way relationships in Appendix A.

Local and global effective parameters

Local effective parameters are related to a single layer, and global effective parameters account for the accumulated effect of the overburden multiple layers. In the context of our paper, these are the coefficients used to approximate local and global traveltimes to fourth-order accuracy. It has already been noticed (e.g., Al-Dajani et al., 1998) that for a general anisotropic single layer, vertical (normal incidence) traveltime and eight local effective parameters are needed: three second order and five fourth order parameters. It was then shown that for the particular case of an orthorhombic layer, only three of the five fourth-order parameters are independent, and in principle, six local parameters suffice. However, the global effective model of multilayer orthorhombic media, with different vertical symmetry planes at each layer, can no longer be considered orthorhombic. There is no common global vertical symmetry plane (or two vertical planes that are perpendicular to each other). Because the symmetry of the horizontal plane is preserved, the global effective model can be considered kinematically equivalent to monoclinic (to fourth-order accuracy); therefore, eight global effective parameters are required.

In this paper, we propose using eight newly defined local and global parameters, indicated by lowercase and uppercase symbols, respectively. These parameters are generic, and they are the same for the slowness-azimuth and offset-azimuth domains. Moreover, they enable performing forward and inverse Dix-type transformations in a straightforward summation and subtraction manner. The forward Dix-type transform provides the global effective parameters by summation over the local parameters, whereas the Dix-type inversion involves subtracting the global effective parameters related to the top and bottom horizons of the given layers.

Second- and fourth-order NMO velocities for traveltime versus horizontal slowness

We define the slowness-azimuth/slowness and the offset-azimuth/slowness domains, second- and fourth-order NMO velocities, $V_{2,\text{slw}}(\psi)$ and $V_{4,\text{slw}}(\psi)$, as the coefficients of the horizontal-slowness square and quad, respectively, of the traveltime series approximation,

$$\frac{t(\psi, p_h) - t_0}{t_0} = V^2_{2,\text{slw}}(\psi) p_h^2 + \frac{1}{2} V^4_{4,\text{slw}}(\psi) p_h^4 + O(p_h^6), \quad (1)$$

where p_h is the slowness azimuth, t_o is the two-way vertical time, and ψ is either the slowness azimuth $\psi = \psi_{slw}$ or the offset azimuth $\psi = \psi_{off}$.

Second-order NMO velocity and quartic coefficient for traveltime versus offset

The asymptotic traveltime approximation, first suggested by Tsvankin and Thomsen (1994) for VTI layered media, has been widely used for azimuthal anisotropy as well (Xu et al., 2005; Vasconcelos and Tsvankin, 2006):

$$t^2(\psi,h) = t_o^2 + \frac{h^2}{V_{2,off}^2(\psi)} + \frac{1}{V_{2,off}^2(\psi)} \cdot \frac{A_{4,off}(\psi)h^4}{V_{2,off}^2(\psi)t_o^2 + \alpha(\psi)h^2}, \quad (2)$$

where h is the offset, t_o is the two-way vertical time, $V_{2,off}(\psi) = V_{nmo}(\psi)$ is the global second-order NMO velocity, $A_{4,off}(\psi)$ is the normalized quartic coefficient, and ψ is either the slowness azimuth or the offset azimuth. Equation 2 can be used to approximate the traveltime in the slowness-azimuth/offset and the offset-azimuth/offset domains. The approximation formula in equation 2 includes a correction factor α in the denominator of the nonhyperbolic term, which makes it possible to achieve reasonable accuracy up to moderate offsets. However, this term has no effect on the fourth-order series approximation for infinitesimal offsets, which can be expressed as

$$t^2(\psi,h) = t_o^2 + \frac{h^2}{V_{2,off}^2(\psi)} + \frac{A_{4,off}(\psi)h^4}{V_{2,off}^4(\psi)t_o^2} + O(h^6). \quad (3)$$

Following, for example, Vasconcelos and Tsvankin (2006), the second- and fourth-order coefficients are symbolically defined by

$$\frac{1}{V_{2,off}^2(\psi)} = \frac{d(t^2)}{d(h^2)}\bigg|_{h=0}, \qquad \frac{A_{4,off}(\psi)}{V_{2,off}^4(\psi)t_o^2} = \frac{1}{2}\frac{d}{d(h^2)}\frac{d(t^2)}{d(h^2)}\bigg|_{h=0}. \quad (4)$$

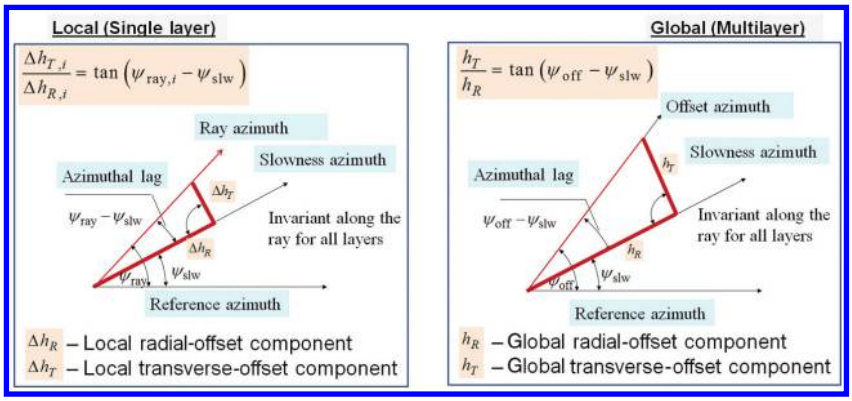

Figure 1. Scheme for local and global radial and transverse offset components with azimuthal lag between the offset azimuth and the slowness azimuth.

The term "symbolically" is used because there is no explicit expression for $t^2(\psi,h)$. We therefore suggest alternative equivalent definitions for $V_{2,off}$ and $A_{4,off}$, which require explicit expression of the two offset components and the traveltime versus the invariant slowness azimuth and horizontal slowness of the incident and reflected waves. To achieve this goal, we suggest first defining the two offset components in the following natural system.

Radial and transverse offset components

It is convenient to split the offset h into two natural components: radial h_R, along the slowness azimuth ψ_{slw}, and transverse h_T, in the normal direction, $\psi_{slw} + \pi/2$, as shown in the scheme of Figure 1, where $h^2 = h_R^2 + h_T^2$. A right triangle is shown in red, whose legs are h_R and h_T. Leg h_R is in line with the slowness azimuth ψ_{slw}, and the hypotenuse h is in line with the offset azimuth ψ_{off}. The acute angle adjacent to leg h_R is the azimuthal lag $\psi_{off} - \psi_{slw}$. We define the "global propagation components" as the global radial and transverse offset components h_R, h_T and the traveltime. The propagation components are computed as functions of azimuth ψ (ψ_{slw} or ψ_{off}) and the horizontal-slowness magnitude p_h,

$$h_R = h_R(\psi,p_h), \quad h_T = h_T(\psi,p_h), \quad t = t(\psi,p_h), \quad (5)$$

by a straightforward summation of the contributions of the individual layers. In part 1, the propagation components are computed in the slowness-azimuth/slowness domain, and in part 2 they are computed in the offset-azimuth/slowness domain.

Proposed definitions for second- and fourth-order NMO velocities, quartic coefficient, and effective anellipticity for traveltime versus offsets.

Using equation 5, the symbolic definitions of the second-order NMO velocity $V_2(\psi)$ and the quartic coefficient $A_4(\psi)$ in equation 4 may be replaced by the equivalent definitions:

$$V_{2,off}^2(\psi) = \lim_{p_h\to 0}\frac{h_R^2 + h_T^2}{t^2 - t_o^2},$$
$$A_{4,off}(\psi) = V_{2,off}^2 t_o^2 \cdot \lim_{p_h\to 0}\frac{(t^2 - t_o^2)V_{2,off}^2 - (h_R^2 + h_T^2)}{(h_R^2 + h_T^2)^2}. \quad (6)$$

We provide explicit expressions for $A_{4,off}(\psi)$, first for the slowness-azimuth domain $\psi = \psi_{slw}$ (part 1) and then for the offset-azimuth domain $\psi = \psi_{off}$ (part 2). Note that $V_2(\psi)$, for all azimuth domains, are already known functions. In part 1, to obtain the explicit expressions for $V_{2,off}(\psi_{slw})$ and $A_{4,off}(\psi_{slw})$ in the slowness-azimuth/offset domain, we first obtain explicit expressions for $h_R(\psi_{slw},p_h), h_T(\psi_{slw},p_h)$, and $t(\psi_{slw},p_h)$ to fourth-order accuracy in the slowness-azimuth/slowness domain, and then we introduce the results in the definitions of equation 6. Furthermore, by making an analogy with the conventional definition arising from VTI layered media (e.g., Gerea et al., 2000), the azimuthally dependent quartic coefficient $A_4(\psi)$ and the corresponding global effective anellipticity

$\eta_{\text{eff}}(\psi)$ (for horizontal slowness and offset) can be similarly defined as

$$A_4(\psi) = -\frac{V_4^4(\psi) - V_2^4(\psi)}{4V_2^4(\psi)},$$
$$\eta_{\text{eff}}(\psi) = \frac{V_4^4(\psi) - V_2^4(\psi)}{8V_2^4(\psi)},$$
$$A_4(\psi) = -2\eta_{\text{eff}}(\psi), \tag{7}$$

so that the fourth-order NMO velocity becomes

$$V_4^4(\psi) = V_2^4(\psi)[1 - 4A_4(\psi)] = V_2^4(\psi)[1 + 8\eta_{\text{eff}}(\psi)]. \tag{8}$$

The NMO velocities and the azimuth in equations 7 and 8 are generic, and these equations are valid in the slowness-azimuth and offset-azimuth domains and for horizontal-slowness and offset components.

Wave types

In this paper, we consider all types of pure-mode and converted waves. For horizontally layered elastic orthorhombic (and also monoclinic) models in which all layers share the same horizontal symmetry plane, the traveltime function can still be expressed as an even function of the offsets or horizontal slowness, in which the reciprocity principle holds for the pure-mode and converted waves: Swapping the source and receiver locations does not change the total traveltime.

METHOD

Our derivation is primarily based on the dependency of body waves propagating through a package of elastic orthorhombic layers (with varying azimuths of vertical symmetry planes) on the invariant slowness azimuth ψ_{slw}. For nearly vertical rays, the incident and reflection angles (or the corresponding horizontal-slowness components) are assumed to be small. Thus, the horizontal-slowness components p_1 and p_2 (or alternatively, the magnitude and azimuth of the horizontal slowness, p_h and ψ_{slw}) can be used as parameters in a fourth-order series approximation of the three propagation components: the two offset components and the traveltime. To approximate the offset components and the traveltime, ray velocity components are needed, in which the latter depend on the vertical-slowness p_3 and its derivatives with respect to the horizontal-slowness components p_1 and p_2 (Grechka et al., 1997; Stovas, 2015).

Our method consists of two main stages:

1) Obtaining local effective parameters for a single orthorhombic layer: Vertical-slowness surface, ray velocity components, and coefficients for the series expansion of local radial and transverse offsets and traveltime.
2) Obtaining global effective parameters for a multilayer orthorhombic model: Dix-type transform, global radial and transverse offsets and traveltime, global second- and fourth-order NMO velocity functions (and hence the effective anellipticity functions) in the slowness-azimuth/slowness and the slowness-azimuth/offset domains.

LOCAL EFFECTIVE PARAMETERS FOR A SINGLE ORTHORHOMBIC LAYER

Vertical slowness

We formulate the eigenvalue problem for the Christoffel matrix in terms of the slowness components p_1, p_2, p_3. This leads to a cubic equation for p_3^2, where the coefficients are polynomials of p_1 and p_2. Considering near-vertical rays, we assume that the horizontal components p_1 and p_2 are small, and this leads to the following series expansion:

$$p_3^2 = \frac{1}{v_{\text{ver}}^2} - Ap_1^2 - Bp_2^2 + v_{\text{ver}}^2 Cp_1^4 + v_{\text{ver}}^2 Dp_2^4 + v_{\text{ver}}^2 Ep_1^2 p_2^2 + O(p_h^6), \tag{9}$$

where v_{ver} is the vertical velocity for the given wave type and p_h is the magnitude of the horizontal slowness, $p_h^2 = p_1^2 + p_2^2$. Coefficients A, B, C, D, E, derived in Appendix B, depend on the components of the stiffness matrix and the considered wave type.

Ray velocity components

The explicit vertical-slowness surface $p_3(p_1, p_2)$ makes it possible to obtain the Cartesian components of the ray velocity that depend on p_3 and its partial derivatives, $\partial p_3/\partial p_1$ and $\partial p_3/\partial p_2$. The derivation is given in Appendix C, and the result is

$$\frac{v_{\text{ray},1}}{v_{\text{ver}}} = p_1 v_{\text{ver}}(A - 2Cv_{\text{ver}}^2 p_1^2 - Ev_{\text{ver}}^2 p_2^2) + O(p_h^5),$$
$$\frac{v_{\text{ray},2}}{v_{\text{ver}}} = p_2 v_{\text{ver}}(B - 2Dv_{\text{ver}}^2 p_2^2 - Ev_{\text{ver}}^2 p_1^2) + O(p_h^5),$$
$$\frac{v_{\text{ray},3}}{v_{\text{ver}}} = 1 - \frac{Av_{\text{ver}}^2 p_1^2}{2} - \frac{Bv_{\text{ver}}^2 p_2^2}{2} + \frac{12C - A^2}{8} v_{\text{ver}}^4 p_1^4 + \frac{12D - B^2}{8} v_{\text{ver}}^4 p_2^4 + \frac{6E - AB}{4} v_{\text{ver}}^4 p_1^2 p_2^2 + O(p_h^6). \tag{10}$$

Local radial and transverse offsets and traveltime

The ray velocity vector makes it possible to compute the local (layer) radial and transverse offset components and local traveltime,

$$\frac{\Delta h_{R,i}}{\Delta z_i} = \frac{\Delta h_{L,i}}{v_{\text{ver},i}\Delta t_{\text{o},i}} = \frac{+v_{\text{ray},1,i}\cos(\psi_{\text{slw}} - \psi_{x_1,i}) + v_{\text{ray},2,i}\sin(\psi_{\text{slw}} - \psi_{x_1,i})}{v_{\text{ray},3,i}},$$
$$\frac{\Delta h_{T,i}}{\Delta z_i} = \frac{\Delta h_{T,i}}{v_{\text{ver},i}\Delta t_{\text{o},i}} = \frac{-v_{\text{ray},1,i}\sin(\psi_{\text{slw}} - \psi_{x_1,i}) + v_{\text{ray},2,i}\cos(\psi_{\text{slw}} - \psi_{x_1,i})}{v_{\text{ray},3,i}},$$
$$\frac{\Delta t_i}{\Delta z_i} = \frac{\Delta t_i}{v_{\text{ver},i}\Delta t_{\text{o},i}} = \frac{1}{v_{\text{ray},3,i}}, \tag{11}$$

where ψ_{x_1} is the azimuth of the local orthorhombic axis x_1 and we use the symbol Δ to indicate the local (layer) parameters (see Appendix D for details). Next, we combine equations 9–11 to obtain the series expansion of the local offset components and local traveltime

in terms of horizontal slowness and its azimuth. We reduce the powers and products of the trigonometric functions into functions of multiple angles, as the latter are linearly independent. The resulting series are

$$\begin{aligned}
\Delta h_{R,i} &= (u_{2,i} + w_{2x,i}\cos 2\psi_{\text{slw}} + w_{2y,i}\sin 2\psi_{\text{slw}})p_h \\
&\quad + (u_{4,i} + w_{42x,i}\cos 2\psi_{\text{slw}} + w_{42y,i}\sin 2\psi_{\text{slw}} \\
&\quad + w_{44x,i}\cos 4\psi_{\text{slw}} + w_{44y,i}\sin 4\psi_{\text{slw}})p_h^3 + O(p_h^5), \\
\Delta h_{T,i} &= -(w_{2x,i}\sin 2\psi_{\text{slw}} p_h - w_{2y,i}\cos 2\psi_{\text{slw}})p_h \\
&\quad - \left(\frac{1}{2}w_{42x,i}\sin 2\psi_{\text{slw}} - \frac{1}{2}w_{42y,i}\cos 2\psi_{\text{slw}}\right. \\
&\quad \left. + w_{44x,i}\sin 4\psi_{\text{slw}} - w_{44y,i}\cos 4\psi_{\text{slw}}\right)p_h^3 + O(p_h^5), \\
\Delta t_i - \Delta t_{\text{o},i} &= \frac{1}{2}(u_{2,i} + w_{2x,i}\cos 2\psi_{\text{slw}} + w_{2y,i}\sin 2\psi_{\text{slw}})p_h^2 \\
&\quad + \frac{3}{4}(u_{4,i} + w_{42x,i}\cos 2\psi_{\text{slw}} + w_{42y,i}\sin 2\psi_{\text{slw}} \\
&\quad + w_{44x,i}\cos 4\psi_{\text{slw}} + w_{44y,i}\sin 4\psi_{\text{slw}})p_h^4 + O(p_h^6).
\end{aligned} \tag{12}$$

The coefficients of these series represent the local effective parameters. The second-order parameters u_2, w_{2x}, w_{2y} and fourth-order parameters $u_4, w_{42x}, w_{42y}, w_{44x}, w_{44y}$ are described in Appendix D. They depend on the wave type, elastic properties, azimuth of the vertical symmetry planes, and thickness of the layer.

GLOBAL EFFECTIVE PARAMETERS FOR A MULTILAYER MODEL

Forward and inverse Dix-type transforms

One of the main strengths of our method is that the forward and inverse Dix-type transforms become simple summation and subtraction operations, respectively. The global effective parameters can be obtained by a straightforward Dix-type summation over the local effective parameters:

$$\begin{aligned}
&U_{2,n} = \sum_{i=1}^{n} u_{2,i}, \quad W_{2x,n} = \sum_{i=1}^{n} w_{2x,i}, \quad W_{2y,n} = \sum_{i=1}^{n} w_{2y,i}, \\
&U_{4,n} = \sum_{i=1}^{n} u_{4,i}, \quad W_{42x,n} = \sum_{i=1}^{n} w_{42x,i}, \quad W_{42y,n} = \sum_{i=1}^{n} w_{42y,i}, \\
&W_{44x,n} = \sum_{i=1}^{n} w_{44x,i}, \quad W_{44y,n} = \sum_{i=1}^{n} w_{44y,i}.
\end{aligned} \tag{13}$$

The local effective parameters are related to the individual layers (and include indices of the layers), whereas the global parameters are related to all the layers above the indicated horizons (and include indices of the bottom horizons). Should we stack all n layers of the model, the global effective model will be related to the lowermost horizon. For the global effective model of horizon m, we stack the first m layers. It is important to note that the proposed Dix-type approach is generic and can be implemented for any type of anisotropic layered model in which the reciprocity principle still holds. In other words, the type of anisotropic symmetry is only relevant for computation of the eight local effective parameters of each layer, whereas computation of the eight global effective parameters is generic.

Although inversion is beyond the scope of this paper, we show that by subtracting the eight global effective parameters related to two successive top and bottom horizons, we obtain the local effective parameters of the layer confined between these two horizons. This operation may be considered as the generalized Dix inversion:

$$\begin{aligned}
&u_{2,i} = U_{2,i} - U_{2,i-1}, \quad w_{2x,i} = W_{2x,i} - W_{2x,i-1}, \\
&w_{2y,i} = W_{2y,i} - W_{2y,i-1}, \quad u_{4,i} = U_{4,i} - U_{4,i-1}, \\
&w_{42x,i} = W_{42x,i} - W_{42x,i-1}, \quad w_{42y,i} = W_{42y,i} - W_{42y,i-1}, \\
&w_{44x,i} = W_{44x,i} - W_{44x,i-1}, \quad w_{44y,i} = W_{44y,i} - W_{44y,i-1}.
\end{aligned} \tag{14}$$

Note that at the free surface, the global parameters are all zero. The vertical time in the relationships for the local effective parameters is two way for pure-mode waves and one way in the case of converted waves. For converted waves, all layers have to be passed twice (for incident and reflected waves) when stacking the local effective parameters into the global ones.

Global radial and transverse offsets and traveltime

Here, we compute the global (multilayer) radial and transverse components of the offset, h_R, h_T, along and across the slowness azimuth, respectively, and the global (total) traveltime. The method is generic and can be implemented for any type of anisotropy and any wave type, provided the reciprocity principle holds. Therefore, the traveltime is an even function of the offset or horizontal slowness.

We define the azimuthally anisotropic global effective medium as a single layer that has the same total vertical time t_{o} as the multilayer model and provides the same reflection traveltime t and the same offset components (for a given accuracy) for any slowness azimuth. With the hyperbolic approximation, the identity holds up to (including) the linear terms of order p_h for offset components, and up to the quadratic terms of order p_h^2 for the reflection traveltime. With the nonhyperbolic approximation, the identity holds up to the third-order terms p_h^3 for the offset components, and up to the fourth-order terms p_h^4 for the traveltime. Because the slowness azimuth is identical for all layers, the local radial and transverse offset components, $\Delta h_{R,i}$ and $\Delta h_{T,i}$, can be added separately through all the individual layers. The local traveltimes Δt_i are added as well. Contrarily, the resulting horizontal propagation $\Delta h_i = \sqrt{\Delta h_{R,i}^2 + \Delta h_{T,i}^2}$ cannot be added because the azimuth of the ray velocity in the different layers varies. The global offset components and traveltime for an overburden layered model consisting of n layers are then obtained by straightforward summation:

$$h_{R,n} = \sum_{i=1}^{n} \Delta h_{R,i}, \quad h_{T,n} = \sum_{i=1}^{n} \Delta h_{T,i}, \quad t_n = \sum_{i=1}^{n} \Delta t_{,i}. \tag{15}$$

The slowness-azimuth domain global offset components and total traveltime can also be expressed in terms of the global effective parameters presented in equation 13:

$$
\begin{aligned}
&h_{R,n}(\psi_{\mathrm{slw}},p_h)\\
&=(U_{2,n}+W_{2x,n}\cos 2\psi_{\mathrm{slw}}+W_{2y,n}\sin 2\psi_{\mathrm{slw}})p_h\\
&+(U_{4,n}+W_{42x,n}\cos 2\psi_{\mathrm{slw}}+W_{42y,n}\sin 2\psi_{\mathrm{slw}}\\
&+W_{44x,n}\cos 4\psi_{\mathrm{slw}}+W_{44y,n}\sin 4\psi_{\mathrm{slw}})p_h^3+O(p_h^5),\\
&h_{T,n}(\psi_{\mathrm{slw}},p_h)\\
&=-(W_{2x,n}\sin 2\psi_{\mathrm{slw}}-W_{2y,n}\cos 2\psi_{\mathrm{slw}})p_h\\
&-\left(\frac{1}{2}W_{42x,n}\sin 2\psi_{\mathrm{slw}}-\frac{1}{2}W_{42y,n}\cos 2\psi_{\mathrm{slw}}\right.\\
&\left.+W_{44x,n}\sin 4\psi_{\mathrm{slw}}-W_{44y,n}\cos 4\psi_{\mathrm{slw}}\right)p_h^3+O(p_h^5),\\
&t_n(\psi_{\mathrm{slw}},p_h)=t_{\mathrm{o},n}+\overbrace{\tfrac{1}{2}(U_{2,n}+W_{2x,n}\cos 2\psi_{\mathrm{slw}}+W_{2y,n}\sin 2\psi_{\mathrm{slw}})}^{V^2_{2,\mathrm{slw}}(\psi_{\mathrm{slw}})t_{\mathrm{o},n}}p_h^2\\
&+\overbrace{\tfrac{3}{4}(U_{4,n}+W_{42x,n}\cos 2\psi_{\mathrm{slw}}+W_{42y,n}\sin 2\psi_{\mathrm{slw}}+W_{44x,n}\cos 4\psi_{\mathrm{slw}}+W_{44y,n}\sin 4\psi_{\mathrm{slw}})}^{1/2V^4_{4,\mathrm{slw}}(\psi_{\mathrm{slw}})t_{\mathrm{o},n}}p_h^4+O(p_h^6).
\end{aligned}
\tag{16}
$$

It follows from the last equation for traveltime that the second- and fourth-order NMO velocities in the slowness-azimuth/slowness domain, for a given horizon index n, are

$$
\begin{aligned}
V_2^2(\psi_{\mathrm{slw}}) &= \frac{U_{2,n}+W_{2x,n}\cos 2\psi_{\mathrm{phs}}+W_{2y,n}\sin 2\psi_{\mathrm{phs}}}{t_{\mathrm{o},n}}\\
V_4^4(\psi_{\mathrm{slw}}) &= \frac{2}{t_{\mathrm{o},n}}(U_{4,n}+W_{42x,n}\cos 2\psi_{\mathrm{slw}}\\
&\quad +W_{42y,n}\sin 2\psi_{\mathrm{slw}}+W_{44x,n}\cos 4\psi_{\mathrm{slw}}\\
&\quad +W_{44y,n}\sin 4\psi_{\mathrm{slw}}).
\end{aligned}
\tag{17}
$$

This may be also arranged as

$$
\begin{aligned}
V^2_{2,\mathrm{slw}}(\psi_{\mathrm{slw}}) &= V^2_{2,\mathrm{H}}\cos^2 2(\psi_{\mathrm{slw}}-\Psi_{2,\mathrm{H}})\\
&\quad +V^2_{2,\mathrm{L}}\sin^2 2(\psi_{\mathrm{slw}}-\Psi_{2,\mathrm{H}})\\
V^4_{4,\mathrm{slw}}(\psi_{\mathrm{slw}}) &= \bar{V}_4^4+\frac{V^4_{4,\mathrm{H}}-V^4_{4,\mathrm{L}}}{2}\frac{\cos 2(\psi_{\mathrm{slw}}-\Psi_{42})}{\cos 2\Delta\Psi_{42}}\\
&\quad +\frac{V^4_{4,\mathrm{H}}-2\bar{V}_4^4+V^4_{4,\mathrm{L}}}{2}\frac{\cos 4(\psi_{\mathrm{slw}}-\Psi_{44})}{\cos 4\Delta\Psi_{44}}.
\end{aligned}
\tag{18}
$$

The first equation in 18, for the second-order NMO velocity in the slowness-azimuth/slowness domain, is a known function (e.g., Stovas, 2015). The high and low second-order NMO velocities, $V_{2,\mathrm{H}}$ and $V_{2,\mathrm{L}}$, and the azimuth $\Psi_{2,\mathrm{H}}$ of the high second-order NMO velocity are defined by

$$
\begin{aligned}
V^2_{2,\mathrm{H}} &= \frac{U_2+W_2}{t_{\mathrm{o}}}, \quad V^2_{2,\mathrm{L}} = \frac{U_2-W_2}{t_{\mathrm{o}}},\\
\cos 2\Psi_{2,\mathrm{H}} &= \frac{W_{2x}}{W_2}, \quad \sin 2\Psi_{2,\mathrm{H}} = \frac{W_{2y}}{W_2},\\
W_2 &= \sqrt{W_{2x}^2+W_{2y}^2}.
\end{aligned}
\tag{19}
$$

Two additional fourth-order global azimuths Ψ_{42} and Ψ_{44} and their corresponding residuals appear in the second equation in 18:

$$
\begin{aligned}
&\cos 2\Psi_{42} = \frac{W_{42x}}{W_{42}}, \quad \sin 2\Psi_{42} = \frac{W_{42y}}{W_{42}},\\
&W_{42} = \pm\sqrt{W_{42x}^2+W_{42y}^2}, \quad \cos 4\Psi_{44} = \frac{W_{44x}}{W_{44}},\\
&\sin 4\Psi_{44} = \frac{W_{44y}}{W_{44}}, \quad W_{44} = \pm\sqrt{W_{44x}^2+W_{44y}^2},
\end{aligned}
\tag{20}
$$

where the residual azimuths are

$$
\Delta\Psi_{42} = \Psi_{42}-\Psi_{2,\mathrm{H}}, \quad \Delta\Psi_{44} = \Psi_{44}-\Psi_{2,\mathrm{H}}. \tag{21}
$$

Parameter $\bar{V}_4$ is the so-called azimuthally isotropic fourth-order NMO velocity,

$$
\bar{V}_4^4 = 2U_4/t_{\mathrm{o}}, \tag{22}
$$

where t_{o} is the two-way vertical time. Parameter W_2 defined in equation 19 is always positive. The signs of W_{42} and W_{44} are chosen so that the fourth-order azimuths Ψ_{42} and Ψ_{44} are the closest to the azimuth $\Psi_{2,\mathrm{H}}$, where for a single-layer model, $\Psi_{42}=\Psi_{44}=\Psi_{2,\mathrm{H}}$. Therefore, the following range constraint holds:

$$
\begin{aligned}
|\Psi_{2,\mathrm{H}}| &< \pi/2 = 90^{\mathrm{o}},\\
|\Delta\Psi_{42}| &< \pi/4 = 45^{\mathrm{o}},\\
|\Delta\Psi_{44}| &< \pi/8 = 22.5^{\mathrm{o}}.
\end{aligned}
\tag{23}
$$

We emphasize that $V_{2,\mathrm{H}}$ and $V_{2,\mathrm{L}}$ are the highest and lowest second-order NMO velocities, respectively, whereas this is not true for $V_{4,\mathrm{H}}$ and $V_{4,\mathrm{L}}$, which are the fourth-order NMO velocities that correspond to the azimuths of the high and low second-order NMO velocities, respectively,

$$
V_{4,\mathrm{H}} = V_4(\Psi_{2,\mathrm{H}}), \quad V_{4,\mathrm{L}} = V_4(\Psi_{2,\mathrm{L}}), \quad \Psi_{2,\mathrm{L}} = \Psi_{2,\mathrm{H}}+\pi/2. \tag{24}
$$

Moreover, it is not necessarily true that $V_{4,\mathrm{H}} > V_{4,\mathrm{L}}$, and for a multilayer medium, $V_{4,\mathrm{H}}$ and $V_{4,\mathrm{L}}$ are not the extreme values of function $V_4(\psi)$. For a single layer, these are extreme values because of the existence of the vertical symmetry planes. It is interesting to note that not only $V_{2,\mathrm{H}}$ and $V_{2,\mathrm{L}}$, but also $V_{4,\mathrm{H}}$ and $V_{4,\mathrm{L}}$ accept identical values in all azimuthal domains.

Slowness-azimuth/offset domain second-order NMO velocity

Introducing equation 4 into the first equation of definition 5, we obtain the global second-order NMO velocity that matches the result obtained by Koren and Ravve (2014) and Stovas (2015) in the slowness-azimuth/offset domain:

$$
V^2_{2,\mathrm{off}}(\psi_{\mathrm{slw}}) = \frac{V^4_{2,\mathrm{H}}\cos^2(\psi_{\mathrm{slw}}-\Psi_{2,\mathrm{H}})+V^4_{2,\mathrm{L}}\sin^2(\psi_{\mathrm{slw}}-\Psi_{2,\mathrm{H}})}{V^2_{2,\mathrm{H}}\cos^2(\psi_{\mathrm{slw}}-\Psi_{2,\mathrm{H}})+V^2_{2,\mathrm{L}}\sin^2(\psi_{\mathrm{slw}}-\Psi_{2,\mathrm{H}})}, \tag{25}
$$

where $V_{2,\mathrm{H}}$, $V_{2,\mathrm{L}}$, and $\Psi_{2,\mathrm{H}}$ are the high and low global second-order NMO velocities and the azimuth of the high second-order NMO velocity, respectively, defined in equation 19, and t_{o} is the two-way vertical time for the entire multilayer package.

Slowness-azimuth/offset-domain fourth-order NMO velocity

Substituting equation 16 into the second equation of definition 6 and using equation 8, we obtain the desired azimuthally dependent global fourth-order NMO velocity function, presented in a compact way as a product of a normalizing factor $K_{2,\text{off}}(\psi_{\text{slw}})$ and a kernel $K_{4,\text{off}}(\psi_{\text{slw}})$:

$$V^4_{4,\text{off}}(\psi_{\text{slw}}) = K_{2,\text{off}}(\psi_{\text{slw}})K_{4,\text{off}}(\psi_{\text{slw}}). \tag{26}$$

The normalizing factor $K_{2,\text{off}}(\psi_{\text{slw}})$ depends solely on the global effective second-order parameters, whereas the kernel $K_{4,\text{off}}(\psi_{\text{slw}})$ depends on the effective second-order and fourth-order parameters. The full derivation of $K_{2,\text{off}}(\psi_{\text{slw}})$ and $K_{4,\text{off}}(\psi_{\text{slw}})$ is given in Appendix E. For any slowness azimuth, the fourth-order kernel is a scalar value presented in bilinear form

$$K_{4,\text{off}}(\psi_{\text{slw}}) = \mathbf{m}\mathbf{M}_{\text{slw/off}}\mathbf{a}_{\text{slw},7}, \tag{27}$$

where $\mathbf{m}$ is a row vector that includes the five fourth-order global effective parameters, $\mathbf{M}_{\text{slw/off}}$ is a 5×7 matrix that depends solely on the second-order global effective parameters, and $\mathbf{a}_{\text{slw},7}$ is a column vector of length 7 that depends on the slowness azimuth alone.

NUMERICAL EXAMPLE FOR A SINGLE LAYER AND A PACKAGE OF LAYERS

To test the validity of our derived formulas, we introduce our newly derived azimuthally dependent global fourth-order NMO velocity (or corresponding effective anellipticity) into equation 2. For P-waves in VTI-layered media, Alkhalifah and Tsvankin (1995) suggest approximating the correction factor α in the denominator of the nonhyperbolic term by

$$\alpha = 1 + 2\eta_{\text{eff}}. \tag{28}$$

Table 1. Elastic properties of a single-layer orthorhombic medium.

δ_1	δ_2	δ_3	ε_1	ε_2	γ_1	γ_2	f	v_P	Δz	ψ_{x_1}
0.25	0.10	−0.05	0.30	0.15	0.12	−0.05	0.75	3.5	0.5	0

To approximate the traveltimes as functions of offsets in layered orthorhombic media, we follow the concepts presented by Vasconcelos and Tsvankin (2006), but in the slowness-azimuth domain (rather than the offset-azimuth domain), with azimuthally dependent effective anellipticity $\eta_{\text{eff}} = \eta_{\text{eff}}(\psi_{\text{slw}})$. To demonstrate the importance of the fourth-order term, we compare the accuracy of the hyperbolic and nonhyperbolic moveout approximations, first with a single-layer (homogeneous) orthorhombic model, whose properties are listed in Table 1, and then with a multilayer model whose properties are listed in Tables 2 and 3. The nonhyperbolic and hyperbolic traveltime approximations are computed with equation 2, with and without the nonhyperbolic term.

To assign realistic values to the elastic orthorhombic properties of the layers, we track the theory proposed by Schoenberg and Douma (1988) and Schoenberg and Helbig (1997) and further enhanced by Bakulin et al. (2000, 2002). Grechka (2007) demonstrates that the fracture properties are also affected by the background anisotropy (e.g., VTI) and refine the fracture compliances for an arbitrarily anisotropic ellipsoidal inclusion embedded in a homogeneous triclinic host, following Eshelby (1957). In this approach, vertical fractures and horizontal layering are combined to form a long-wavelength equivalent orthorhombic medium. The model was named vertically fractured transverse isotropy (VFTI). Such a medium constitutes a particular case of general orthorhombic media due to the constraint related to the stiffness matrix components:

$$C_{13}(C_{22} + C_{12}) = C_{23}(C_{11} + C_{12}). \tag{29}$$

For weak anisotropy, this constraint simplifies to (Bakulin et al., 2000)

$$4f(1-f)(\gamma_2 - \gamma_1) = f(\delta_2 - \delta_1) + (2f-1)(\varepsilon_2 - \varepsilon_1). \tag{30}$$

Given the elastic properties of the underlying background VTI medium $\delta, \varepsilon, \gamma, f_b, v_{Pb}$ (where subscript b means background) and the weakness of one or two mutually orthogonal vertical fractures, one can establish elastic VFTI properties. Each of the two fracture systems is characterized by three unitless weakness values: vertical tangential weakness Δ_{v}, horizontal tangential Δ_{h}, and normal weakness Δ_{n}. Tables 1 and 2 below show the direction of the normal to the fracture plane. However, following Bakulin et al. (2002), we assume different vertical and horizontal tangential weakness, and in addition to Tsvankin's (1997) parameters (presented in equations 31 and 32), we apply the method to also compute coefficient f and vertical compressional velocity v_P (equation 33):

Table 2. Properties of a background VTI layered model, fracture weakness, and orientation.

Layer	δ	ε	γ	f_b	v_{Pb}	Δz	Δ_{n_1}	Δ_{n_2}	Δ_{v_1}	Δ_{v_2}	Δ_{h_1}	Δ_{h_2}	ψ_{x_1}
1	0.12	0.23	0.07	0.72	2.5	0.6	0.20	0.10	0.23	0.12	0.29	0.15	0
2	0.15	0.30	0.06	0.78	3.0	0.5	0.30	0	0.35	0	0.39	0	30
3	0.05	0.17	0.10	0.75	3.5	0.6	0	0.22	0	0.33	0	0.32	60
4	0.23	0.25	0.06	0.82	3.8	0.7	0.12	0.40	0.16	0.45	0.20	0.50	90
5	0.10	0.20	0.05	0.70	3.2	0.4	0.15	0.16	0.18	0.32	0.20	0.28	120
6	0.12	0.19	0.08	0.80	3.6	0.5	0.0	0.22	0	0.36	0.0	0.25	150

$$\delta_1 = \delta - 2(1-f_b)[(2f_b-1)\Delta_{n_2} + \Delta_{v_2}]$$
$$\delta_2 = \delta - 2(1-f_b)[(2f_b-1)\Delta_{n_1} + \Delta_{v_1}]$$
$$\delta_3 = -2(1-f_b)[(\Delta_{h_1} - \Delta_{n_1}) + (\Delta_{h_2} - \Delta_{n_2}) + 2f_b\Delta_{n_2}] \quad (31)$$

$$\varepsilon_1 = \varepsilon - 2f_b(1-f_b)\Delta_{n_2}, \quad \gamma_1 = \gamma - \frac{\Delta_{h_1} + \Delta_{h_2} - \Delta_{v_1}}{2}$$
$$\varepsilon_2 = \varepsilon - 2f_b(1-f_b)\Delta_{n_1}, \quad \gamma_2 = \gamma - \frac{\Delta_{h_1} + \Delta_{h_2} - \Delta_{v_2}}{2} \quad (32)$$

Table 3. Thickness, orientation, and elastic properties of a VFTI layered model.

Layer	δ_1	δ_2	δ_3	ε_1	ε_2	γ_1	γ_2	f	v_P	Δz	ψ_{x_1}
1	0.028	−0.058	−0.159	0.190	0.149	−0.035	−0.090	0.768	2.426	0.6	0
2	0.150	−0.078	−0.040	0.300	0.197	0.040	−0.135	0.836	2.855	0.5	30
3	−0.170	0.050	−0.215	0.088	0.170	−0.060	0.105	0.736	3.402	0.6	60
4	−0.024	−0.145	−0.301	0.132	0.215	−0.210	−0.065	0.810	3.371	0.7	90
5	−0.130	−0.044	−0.236	0.133	0.137	−0.100	−0.030	0.739	3.120	0.4	120
6	−0.077	0.120	−0.153	0.120	0.190	−0.045	0.135	0.784	3.455	0.5	150

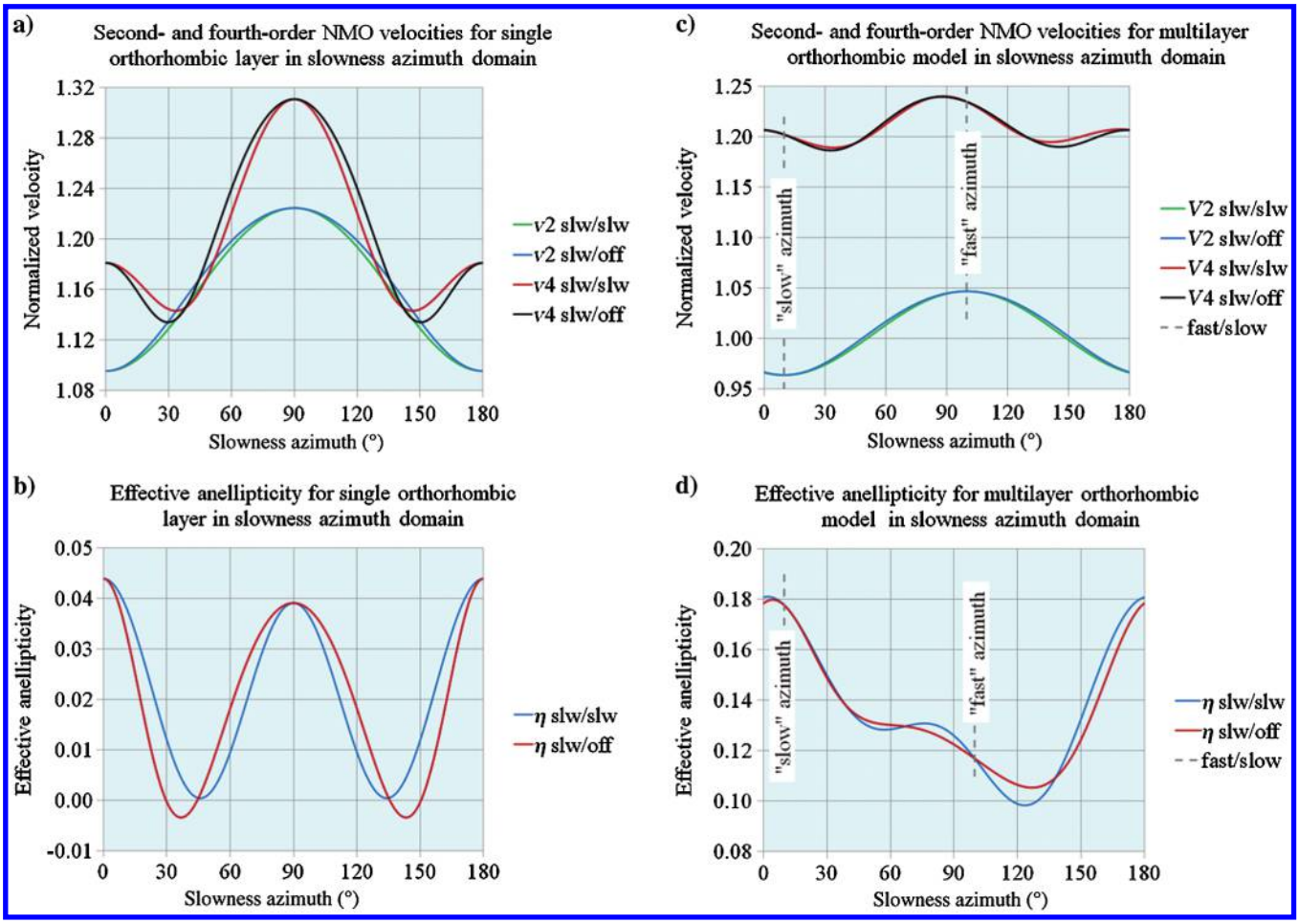

Figure 2. Second- and fourth-order NMO velocities and effective anellipticity for single-layer and multilayer models in the slowness-azimuth domain: (a) Second- and fourth-order NMO velocities for single-layer orthorhombic model in slowness-azimuth/slowness and slowness-azimuth/offset domains, (b) effective anellipticity for single-layer model in slowness-azimuth/slowness and slowness-azimuth/offset domains, (c) second- and fourth-order NMO velocities for multilayer orthorhombic model in the slowness-azimuth/slowness and slowness-azimuth/offset domains, and (d) effective anellipticity for multilayer model in the slowness-azimuth/slowness and slowness-azimuth/offset domains. The medium properties of the single-layer and multilayer models are listed in Tables 1 and 3, respectively. Legend notations "slw/slw" and "slw/off" indicate slowness-azimuth slowness and slowness-azimuth/offset domains, respectively, and legend notation "fast/slow" stand for the azimuths of the high and low second-order NMO velocities.

$$f = f_b + (1-f_b)\Delta_{v_1} - (1-f_b)(2f_b-1)^2(\Delta_{n_1}+\Delta_{n_2})$$
$$v_P^2/v_{Pb}^2 = 1-(2f_b-1)^2(\Delta_{n_1}+\Delta_{n_2}). \quad (33)$$

In Table 2, we list the properties of the background VTI medium, weakness, and azimuth of the normal to the fracture plane ψ_{x_1}, and layer thickness. The corresponding computed properties of the re-

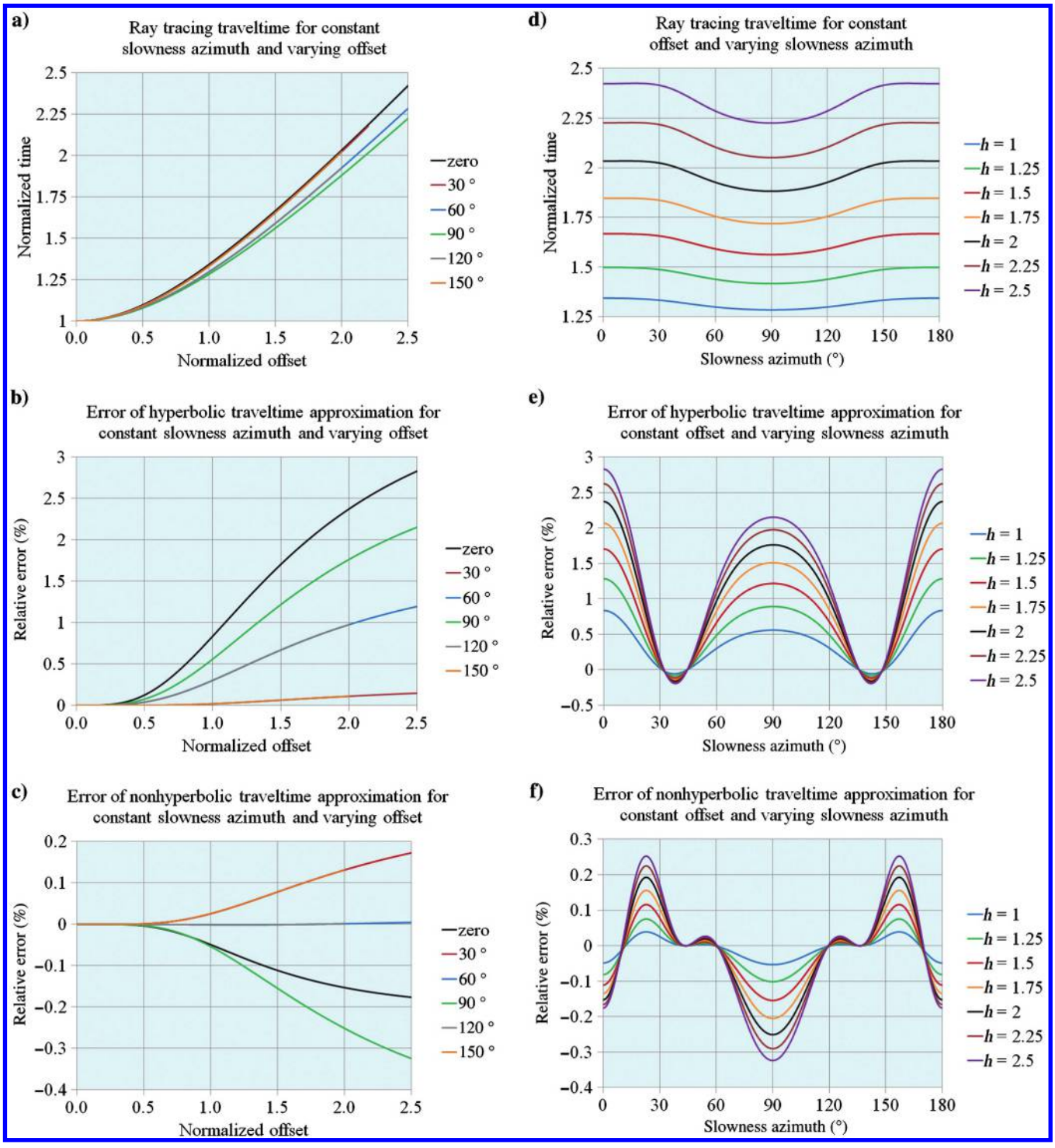

Figure 3. Relative errors of hyperbolic and nonhyperbolic traveltime approximations versus offset magnitude and slowness azimuth, for a single-layer orthorhombic model: (a) Ray tracing traveltime versus offset, for constant slowness azimuth; (b) relative error of hyperbolic traveltime approximation versus offset, for constant slowness azimuth; (c) relative error of nonhyperbolic traveltime approximation versus offset, for constant slowness azimuth; (d) ray tracing traveltime versus slowness azimuth, for constant offset; (e) relative error of hyperbolic traveltime approximation versus slowness azimuth, for constant offset; and (f) relative error of nonhyperbolic traveltime approximation versus slowness azimuth, for constant offset. The medium properties are listed in Table 1.

sulting VFTI layers are presented in Table 3. The interval vertical compressional velocity v_P in the tables is in kilometers per second, the thickness Δz is in kilometers, and the azimuth ψ_{x_1} of local orthorhombic axis x_1 is in degrees. In Figure 2a and 2b, we plot the second- and fourth-order NMO velocities and the effective anellipticity, respectively, for the single orthorhombic layer, in the slowness-azimuth/slowness and the slowness-azimuth/offset domains. We can clearly see two vertical symmetry planes on these plots. At the vertical symmetry planes ψ_{x_1} and $\psi_{x_1} + \pi/2$, the second- and fourth-order NMO velocities in all azimuthal domains are equal. In Figure 2c and 2d, the NMO velocities and effective anellipticities for the multilayer model, Table 3, are plotted in the slowness-azimuth/slowness and the slowness-azimuth/offset domains.

For the "high" and "low" global effective azimuths $\Psi_{2,\mathrm{H}}$ and $\Psi_{2,\mathrm{L}} = \Psi_{2,\mathrm{H}} + \pi/2$, corresponding to the high and low second-order NMO velocities, again, the second- and fourth-order NMO velocities in all azimuthal domains are equal. However, only the plots for the global second-order NMO velocity $V_2(\psi)$ are symmetric because these plots are defined by a single azimuthal parameter: the azimuth of the high second-order NMO velocity $\Psi_{2,\mathrm{H}}$. The plots for the fourth-order NMO velocity are defined by $\Psi_{2,\mathrm{H}}$ and two additional global effective azimuths, Ψ_{42} and Ψ_{44}, related to the fourth-order terms with the azimuth doubled and the azimuth quadrupled, respectively. Unlike homogeneous orthorhombic media, multilayer models with different azimuthal orientations of the orthorhombic symmetry planes at each layer have no common vertical planes of symmetry. Their "equivalent medium" is more likely monoclinic than orthorhombic because the layers share only the horizontal plane of symmetry (and not the vertical ones). The NMO velocities in Figure 2 are normalized (divided by the average vertical velocity $V_{\mathrm{ave}} = 2z/t_{\mathrm{o}}$, where z is the depth of the reflector and t_{o} is the two-way vertical time).

In Figure 3, we plot the exact traveltime $t = t(\psi_{\mathrm{slw}}, h)$ and relative errors for the hyperbolic and nonhyperbolic traveltime approximations in the slowness-azimuth/offset domain for the single-layer model versus offset and slowness azimuth, comparing the approximations with an exact numerical solution. In Figure 3a–3c, the slowness azimuth is kept constant, and the offset magnitude varies. The offset and traveltime are normalized, $\bar{t} = t/t_{\mathrm{o}}$ and $\bar{h} = h/(2z)$, where z is the depth of the reflection point. The offset range is $0 \le \bar{h} \le 2.5$, and the slowness azimuths considered are $\psi_{\mathrm{slw}} = 0^{\mathrm{o}}$, 30^{o}, 60^{o}, 90^{o}, 120^{o}, and 150^{o}. Due to the vertical symmetry planes, we see that the exact solution and approximation errors for the complementary azimuths, ψ_{slw} and $\pi - \psi_{\mathrm{slw}}$, are identical; i.e., plots for 30^{o} and 150^{o} or 60^{o} and 120^{o} look alike.

In Figure 3d–3f, we plot the traveltime and relative traveltime errors for fixed offsets $\bar{h} = 1, \ldots, 2.5$ with a step $\Delta\bar{h} = 0.25$, for continuously varying slowness azimuth, $0 \le \psi_{\mathrm{slw}} \le \pi$. Figure 3a and 3d shows the numerical solution, Figure 3b and 3e shows the relative errors of the hyperbolic approximation, and Figure 3c and 3f shows the relative errors of the nonhyperbolic approximation. In the worst case, the error for the hyperbolic approximation is 2.83%; for the nonhyperbolic approximation, it is much smaller, 0.324%.

The contribution of the nonhyperbolic term is essential to obtaining the required accuracy. It is interesting to note that for this particular model, the azimuthal dependency of the traveltime is relatively weak in the proximity of the azimuths of the high and low NMO velocities.

As we see in Figure 4 (which is a magnification of Figure 3e and 3f combined), for two specific azimuths in the range of $0 \le \psi_{\mathrm{slw}} \le \pi/2$, and corresponding symmetric azimuths in the range of $\pi/2 \le \psi_{\mathrm{slw}} \le \pi$, the accuracies of the hyperbolic and nonhyperbolic approximations are equal for each specific azimuth. At these azimuths, we observe the effective elliptic anisotropy, in which the effective anellipticity term vanishes. In Figure 4, the solid lines are errors of the nonhyperbolic approximation. The dashed lines are the corresponding errors of the hyperbolic approximation. Each color corresponds to a fixed normalized offset (specified in the legend). The effective elliptic anisotropy at $\psi_{\mathrm{slw}} = 29.6^{\mathrm{o}}$ and 44.5^{o} is shown by two vertical gray lines, when the global effective anellipticity η_{eff} vanishes (changes its sign at this point). For $\psi_{\mathrm{slw}} = 44.5^{\mathrm{o}}$, the error of the traveltime approximation becomes very small, compared with the accuracy of our numerical ray tracing. In case of a multilayer model, vanishing global effective anellipticity is less likely, due to an essential positive induced component of local effective anellipticity caused by vertical velocity variations. This phenomenon will be further studied in the offset-azimuth domain in part 2.

In Figure 5, we analyze the accuracy of the hyperbolic and nonhyperbolic traveltime approximations for the multilayer model, Table 3, applying exact numerical ray tracing for comparison. In Figure 5a–5c, the azimuths are kept constant, $\psi_{\mathrm{slw}} = 0, 30^{\mathrm{o}}, 60^{\mathrm{o}}, 90^{\mathrm{o}}, 120^{\mathrm{o}}$, and 150^{o}, and the offset varies continuously in the range of $0 \le \bar{h} \le 2$. In Figure 5d–5f, the offset magnitudes are kept constant, $\bar{h} = 1, \ldots, 2$ with a step $\Delta\bar{h} = 0.25$, and the azimuth runs for all values, $0 \le \psi_{\mathrm{slw}} \le \pi$. Figure 5a and 5d shows the exact ray tracing solution, Figure 5b and 5e shows the relative errors of hyperbolic traveltime approximation, and Figure 5c and 5f shows the relative errors of nonhyperbolic traveltime approximation. For the given multilayer model, within the studied range of offsets $\bar{h} \le 2$ and all azimuths, the maximum traveltime error of the hyperbolic approximation is approximately 11%, whereas that of the nonhyperbolic approximation is 1.32% (for a relatively long offset $\bar{h} = 2$, i.e., $h = 4z$). These results reemphasize the importance of using azimuthally dependent fourth-order NMO velocity (or the quartic coefficient) for analyzing azimuthally anisotropic parameters. The error plots may also be considered as evidence that our derived expression for V_4 is correct.

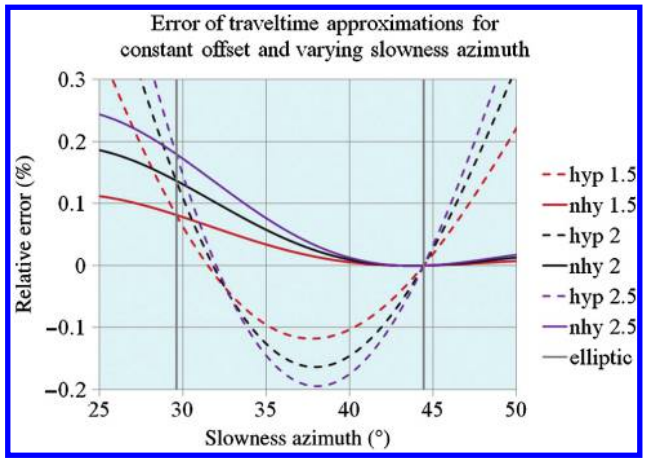

Figure 4. Slowness azimuths of effective elliptic anisotropy, for a single-layer orthorhombic model. The medium properties are listed in Table 1.

DISCUSSION ON CONVERTED WAVES

In the case of converted waves, we compute the local effective parameters of each layer twice: first for the incident wave type and then for the reflected wave type. The one-way vertical time in each case is different. We then stack the local effective parameters into the global effective parameters, passing all layers for both wave types.

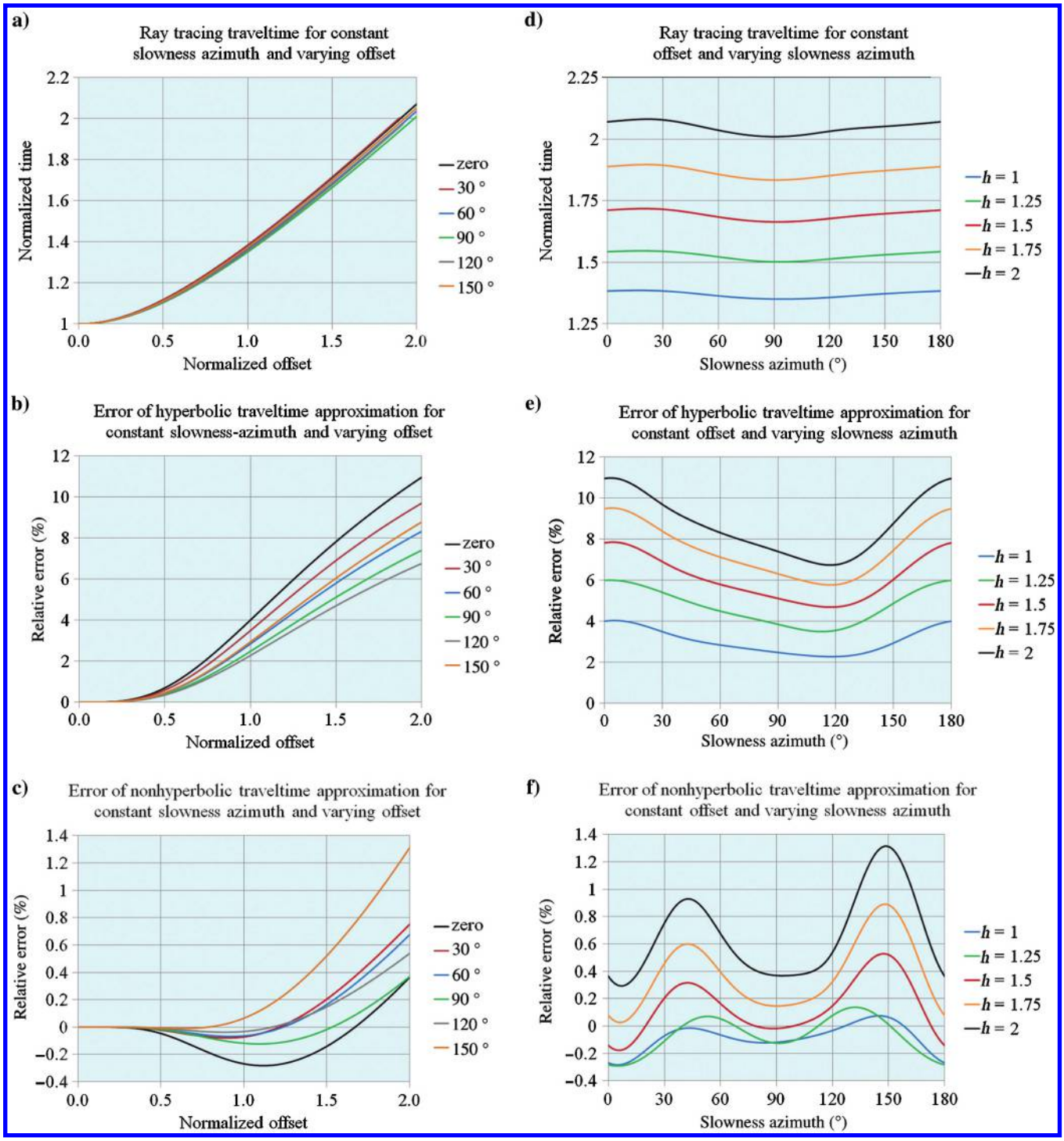

Figure 5. Relative errors of hyperbolic and nonhyperbolic traveltime approximations versus offset magnitude and slowness azimuth, for a multilayer orthorhombic model (VFTI): (a) Ray tracing traveltime versus offset, for constant slowness azimuth; (b) relative error of hyperbolic traveltime approximation versus offset, for constant slowness azimuth; (c) relative error of nonhyperbolic traveltime approximation versus offset, for constant slowness azimuth; (d) ray tracing traveltime versus slowness azimuth, for constant offset; (e) relative error of hyperbolic traveltime approximation versus slowness azimuth, for constant offset; and (f) relative error of nonhyperbolic traveltime approximation versus slowness azimuth, for constant offset. The medium properties are listed in Table 3.

In general, the correction factor α in equation 2 accounts approximately for the effective horizontal velocity of a layered model, and it becomes a key factor in achieving the desired accuracy for moderate to moderately long offsets. This velocity can be approximated with effective anellipticity (equation 28) only for P-waves. For S- and converted waves, equation 28 is not valid. In general, the correction factor should be related to the effective horizontal velocity V_h of the layered model. This approach is suggested by Tsvankin and Thomsen (1994) for VTI, and then it is extended by Al-Dajani and Toksoz (2001), for azimuthally anisotropic layered models,

$$\alpha(\psi) = \frac{2\eta_{\text{eff}}(\psi)V_h^2(\psi)}{V_h^2(\psi) - V_{2,\text{off}}^2(\psi)},$$
$$V_h^4(\psi) = \frac{1}{t_o}\sum_{i=1}^{n}\Delta t_{o,i}v_{h,i}^4(\psi), \tag{34}$$

where $\Delta t_{o,i}$ is the vertical time and $v_{h,i}(\psi)$ is the horizontal ray (group) velocity of an individual layer that corresponds to the given specific azimuth domain used: slowness azimuth or offset azimuth. In their original study, Tsvankin and Thomsen (1994) suggest using the root-mean-square (rms) of horizontal velocities of all layers to compute the effective horizontal velocity. This method is later criticized by Alkhalifah (1997) because for a particular case of layered isotropic media, condition $V_h = V_2$ leads to a total loss of the nonhyperbolic effect (α in equation 34 and thus the whole denominator of the nonhyperbolic term becomes infinite and the nonhyperbolic term vanishes). Therefore, we use the root-mean-four of the individual horizontal velocities, as suggested by Al-Dajani and Toksoz (2001). In addition, the root-mean-four is closer to the maximum value than is the rms, and theoretically, at the infinite offsets, the effective horizontal velocity is that of the layer with the highest velocity.

In the case of compression-to-shear (or shear-to-compression) converted waves, only horizontal velocities of the P-waves have to be summed in the second equation 34, in which local and global vertical times are one-way. The propagation scheme of converted waves with an unbounded offset is presented in Figure 6. This figure is the vertical cross section in the normal incidence plane, i.e., in the vertical plane with the slowness azimuth. Therefore, only radial-offset components are shown in this plane, whereas the transverse components are in the normal vertical plane (rotated 90° from the incidence plane around the vertical axis). Ray angles $\theta_{\text{ray},i}$ shown in this figure are actually their projections on the incidence plane because the ray velocity azimuths $\psi_{\text{ray},i}$ vary from layer to layer.

Consider P-S1 or P-S2 converted waves with a nearly critical opening angle at the reflection point. The opening angle is defined as the angle between the incidence and reflection slowness vectors. Critical angle means that in one of the layers (in the layer with the highest horizontal velocity), the phase and ray velocities become nearly horizontal. Their zenith angles approach 90°, and their azimuths are different. In this case, the two-way offset and the two-way traveltime become unbounded. However, the shear velocities are much slower than the compressional velocities (by about a factor of two or so). Therefore, the zenith angles of the shear slowness vectors are much smaller than the zenith angles for the compressional slowness vectors. In the "highest velocity" layer, only the compressional slowness vector is nearly horizontal; the shear slowness vector is not.

As shown in the scheme in Figure 6, the total offset consists of two legs: the shear leg and the compressional leg. For a nearly critical angle, only the compressional offset leg and its corresponding traveltime become unbounded. The shear offset leg and its corresponding traveltime are bounded. Therefore, in the averaging formula (root-mean-four) for the effective horizontal velocity, only compressional horizontal velocities should be averaged. Similarly, for S1-S2 converted waves (where S1 is the high shear velocity and S2 is the low shear velocity), only the high shear horizontal velocities of the layers should be averaged to obtain the effective horizontal velocity. Overall, we do not expect high accuracy of the traveltime approximation for pure S-waves or shear-to-shear conversion. The existence of triplications and singularities cannot be described by the coefficients computed for the normal incidence ray. Note that although our computed coefficients are exact for all cases, they will be used primarily for pure P-waves and compression-to-shear converted waves.

We note also that, theoretically, the effective horizontal velocity is the horizontal velocity of the high-velocity layer alone. However, such definition — although it leads to correct asymptotic velocity at the infinite offsets — provides an overestimated effective horizontal velocity for finite offsets. Therefore, root-mean-four averaging is a good compromise.

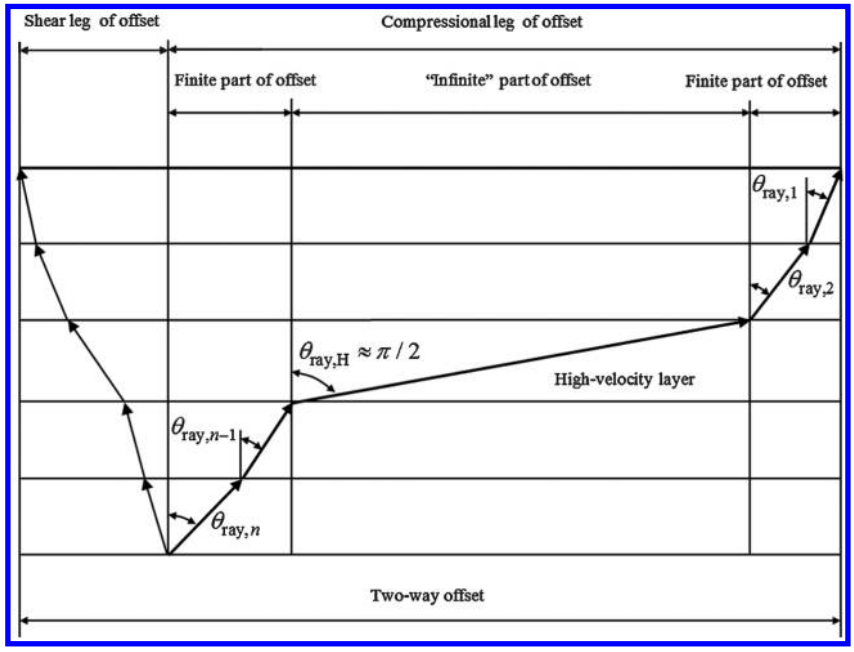

Figure 6. Converted wave propagation scheme in the layered orthorhombic model for unbounded offsets. Vertical incidence plane: Only the radial-offset components are shown. Ray angles $\theta_{\text{ray},i}$ are actually their projections on the incidence plane.

To summarize, the approximation for S- and converted waves requires an explicit computation of the global effective horizontal velocity $V_h(\psi)$. Equation 34 is applicable for all types of waves. However, for P-waves, despite the fact that equation 34 is more accurate, equation 28 can still be used to compute the correction factor because it does not require the additional parameter $V_h(\psi)$.

Finally, we note that the singularity of the vertical S-waves, where $\gamma_1 = \gamma_2$, is beyond the scope of this paper.

CONCLUSIONS

Considering all types of waves, we first derived the expressions for the azimuthally dependent global second- and fourth-order NMO velocity functions for multilayer orthorhombic media in the slowness-azimuth/slowness domain, without making any assumptions about weak anisotropy or acoustic approximation for P-waves. The derivation is based on the computation of natural offset components: radial (along the invariant azimuth of the slowness vector) and transverse (in its perpendicular direction), and the corresponding traveltime as functions of the invariant horizontal slowness within each individual layer. This computation requires a fourth-order approximation of the ray velocity components as a function of the horizontal slowness and its azimuth (slowness azimuth) for near-vertical rays. Using the proposed approach, we obtained three local effective second-order and five local effective fourth-order parameters, which make it possible to obtain the required corresponding eight global effective parameters in a straightforward Dix-type summation. We then derived the slowness-azimuth/offset domain second- and fourth-order NMO velocities that make it possible to approximate the traveltime with respect to offsets, rather than the horizontal slowness. We note that only the computation of the local effective parameters depends on the considered type of anisotropy and wave mode, whereas the Dix-type summation of the eight global effective parameters is generic and can be applied to any general anisotropic layer (including triclinic for pure-mode waves) in the slowness-azimuth and offset-azimuth domains. Comparison between nonhyperbolic asymptotic moveouts computed with the derived azimuthally dependent fourth-order NMO velocity and traveltimes computed by numerical ray tracing shows an excellent match.

ACKNOWLEDGMENTS

The authors are grateful to Paradigm Geophysical for the financial and technical support of this study and for permission to publish its results. We extend our gratitude to reviewers P. Bakker, A. Stovas, Y. Ivanov, and F. Mahmoudian; to associate editor R. Bale; and to assistant editor J. Shragge for their valuable comments and suggestions that helped to improve the content and style of this paper.

APPENDIX A

TWO-WAY RELATIONSHIPS BETWEEN ORTHORHOMBIC STIFFNESS COMPONENTS AND TSVANKIN PARAMETERS

We use Tsvankin's (1997) notations for orthorhombic parameters, which are extensions to the Thomsen (1986) parameters for VTI media. There are nine stiffness parameters that describe the elastic properties of orthorhombic media. The relationships between the density-normalized stiffness matrix components (with Voigt notations) C_{ij} and the dimensionless Tsvankin's parameters are as follows: Two parameters are the vertical compressional velocity v_P and vertical shear velocity v_{S,x_1} (polarized in the direction of the local orthorhombic axis x_1):

$$\begin{aligned} v_P^2 &= C_{33} - \text{vertical compressional velocity},\\ v_{S,x_1}^2 &= C_{55}\\ &\quad - \text{vertical velocity of shear polarized in the } x_1 \text{ direction}. \end{aligned} \tag{A-1}$$

Instead of the vertical shear velocity v_{S,x_1}, one may introduce the dimensionless coefficient:

$$f = \frac{v_P^2 - v_{S,x_1}^2}{v_P^2} = \frac{C_{33} - C_{55}}{C_{33}}. \tag{A-2}$$

The other seven parameters are divided into three groups (Tsvankin, 1997):

1) parameters referring to plane $[x_2, x_3]$

$$\begin{aligned} \varepsilon_1 &= \frac{C_{22} - C_{33}}{2C_{33}}, \quad \gamma_1 = \frac{C_{66} - C_{55}}{2C_{55}},\\ \delta_1 &= \frac{(C_{23} + C_{44})^2 - (C_{33} - C_{44})^2}{2C_{33}(C_{33} - C_{44})} \end{aligned} \tag{A-3}$$

2) parameters referring to plane $[x_1, x_3]$

$$\begin{aligned} \varepsilon_2 &= \frac{C_{11} - C_{33}}{2C_{33}}, \quad \gamma_2 = \frac{C_{66} - C_{44}}{2C_{44}},\\ \delta_2 &= \frac{(C_{13} + C_{55})^2 - (C_{33} - C_{55})^2}{2C_{33}(C_{33} - C_{55})} \end{aligned} \tag{A-4}$$

3) parameter referring to plane $[x_1, x_2]$

$$\delta_3 = \frac{(C_{12} + C_{66})^2 - (C_{11} - C_{66})^2}{2C_{11}(C_{11} - C_{66})}. \tag{A-5}$$

The inverse relationships require additional parameters:

$$A_{12} = C_{12} + C_{66}, \quad A_{13} = C_{13} + C_{55}, \quad A_{23} = C_{23} + C_{44}. \tag{A-6}$$

It is common to assume that A_{12}, A_{13}, and A_{23} are all positive, avoiding anomalous polarization in any of the coordinate planes (Helbig and Schoenberg, 1987; Schoenberg and Helbig, 1997), although this is not a must. The results are

$$\frac{C_{11}}{v_P^2} = 1 + 2\varepsilon_2, \quad \frac{C_{22}}{v_P^2} = 1 + 2\varepsilon_1, \quad \frac{C_{33}}{v_P^2} = 1. \tag{A-7}$$

$$\begin{aligned} \frac{C_{44}}{v_P^2} &= \frac{(1 + 2\gamma_1)(1 - f)}{1 + 2\gamma_2}, \quad \frac{C_{55}}{v_P^2} = 1 - f,\\ \frac{C_{66}}{v_P^2} &= (1 + 2\gamma_1)(1 - f). \end{aligned} \tag{A-8}$$

$$\frac{A_{13}}{v_P^2} = \sqrt{f(f+2\delta_2)} = \sqrt{(1-f)^2 - 2(1+\delta_2)(1-f) + (1+2\delta_2)}. \quad \text{(A-9)}$$

$$\frac{A_{23}}{v_P^2} = \frac{\sqrt{[(1+2\gamma_1)(1-f)-(1+2\gamma_2)]\cdot[(1+2\gamma_1)(1-f)-(1+2\gamma_2)(1+2\delta_1)]}}{1+2\gamma_2}. \quad \text{(A-10)}$$

$$\frac{A_{12}}{v_P^2} = \sqrt{2\delta_3(1+2\varepsilon_2)[(1+2\varepsilon_2)-(1+2\gamma_1)(1-f)]+[(1+2\varepsilon_2)-(1+2\gamma_1)(1-f)]^2}. \quad \text{(A-11)}$$

In the case of acoustic approximation $f = 1$, relationships A-8–A-11 simplify to

$$\frac{C_{13}}{v_P^2} = \sqrt{1+2\delta_2}, \quad \frac{C_{23}}{v_P^2} = \sqrt{1+2\delta_1},$$
$$\frac{C_{12}}{v_P^2} = (1+2\varepsilon_2)\sqrt{1+2\delta_3}, \quad C_{44} = C_{55} = C_{66} = 0. \quad \text{(A-12)}$$

APPENDIX B

VERTICAL SLOWNESS

We derive the function for vertical-slowness $p_3(p_1, p_2)$ for a near-vertical ray, for a single orthorhombic layer with the given elastic properties: the vertical compressional velocity v_P, shear parameter $f = 1 - v_{Sx_1}^2/v_P^2$ (where v_{Sx_1} is the vertical shear velocity related to polarization in the x_1-direction), and Tsvankin's (1997) orthorhombic parameters. All derivations in this appendix are carried out in the local frame of reference attached to the orthorhombic axes of the layer. The Christoffel matrix for the orthorhombic medium is given by Tsvankin (1997). In terms of the slowness components, it may be arranged as (Červený, 2001)

$$\mathbf{\Gamma} = \begin{bmatrix} C_{11}p_1^2+C_{66}p_2^2+C_{55}p_3^2 & (C_{12}+C_{66})p_1p_2 & (C_{13}+C_{55})p_1p_3 \\ (C_{12}+C_{66})p_1p_2 & C_{66}p_1^2+C_{22}p_2^2+C_{44}p_3^2 & (C_{23}+C_{44})p_2p_3 \\ (C_{13}+C_{55})p_1p_3 & (C_{23}+C_{44})p_2p_3 & C_{55}p_1^2+C_{44}p_2^2+C_{33}p_3^2 \end{bmatrix}, \quad \text{(B-1)}$$

where the stiffness components C_{ij} are assumed to be density normalized. The eigenvalue equation for this matrix relates the three slowness components to each other, for three different wave types (compressional, high-velocity shear, and low-velocity shear). All three eigenvalues of $\mathbf{\Gamma}$ are equal to 1:

$$\det(\mathbf{\Gamma} - \mathbf{I}) = 0, \quad \text{(B-2)}$$

where $\mathbf{I}$ is the identity matrix. Introduction of equation B-1 into B-2 results in a cubic equation for the vertical-slowness squared:

$$a p_3^6 + b p_3^4 + c p_3^2 + d = 1, \quad \text{(B-3)}$$

where coefficient a is constant, and the other coefficients are polynomials of horizontal-slowness components p_1 and p_2:

$$a = C_{33}C_{44}C_{45}, \quad \text{(B-4)}$$

$$\begin{aligned} b &= b_o + b_x p_1^2 + b_y p_2^2, \\ b_o &= -C_{33}(C_{44}+C_{55}) - C_{44}C_{55}, \\ b_x &= [C_{11}C_{33} + C_{55}^2 - (C_{13}+C_{55})^2]C_{44} + C_{33}C_{55}C_{66}, \\ b_y &= [C_{22}C_{33} + C_{44}^2 - (C_{23}+C_{44})^2]C_{55} + C_{33}C_{44}C_{66}, \end{aligned} \quad \text{(B-5)}$$

$$\begin{aligned} c &= c_o + c_x p_1^2 + c_y p_2^2 + c_{xx} p_1^4 + c_{yy} p_2^4 + c_{xy} p_1^2 p_2^2, \\ c_o &= C_{33} + C_{44} + C_{55}, \\ c_x &= (C_{13}+C_{55})^2 - (C_{44}+C_{55}+C_{66})C_{55} - C_{11}C_{44} \\ &\quad - (C_{11}+C_{66})C_{33}, \\ c_y &= (C_{23}+C_{44})^2 - (C_{44}+C_{55}+C_{66})C_{44} - C_{22}C_{55} \\ &\quad - (C_{22}+C_{66})C_{33}, \\ c_{xx} &= [C_{11}C_{33} + C_{55}^2 - (C_{13}+C_{55})^2]C_{66} + C_{11}C_{44}C_{55}, \\ c_{yy} &= [C_{22}C_{33} + C_{44}^2 - (C_{23}+C_{44})^2]C_{66} + C_{22}C_{44}C_{55}, \\ c_{xy} &= 2(C_{13}+C_{55})(C_{23}+C_{44})(C_{12}+C_{66}) \\ &\quad + C_{11}C_{22}C_{33} + 2C_{44}C_{55}C_{66} + C_{11}[C_{44}^2 - (C_{23}+C_{44})^2] \\ &\quad + C_{22}[C_{55}^2 - (C_{13}+C_{55})^2] + C_{33}[C_{66}^2 - (C_{12}+C_{66})^2], \end{aligned} \quad \text{(B-6)}$$

$$\begin{aligned} d &= d_x p_1^2 + d_y p_2^2 + d_{xx} p_1^4 + d_{yy} p_2^4 + d_{xy} p_1^2 p_2^2 + d_{xxx} p_1^6 \\ &\quad + d_{yyy} p_2 6 + d_{xxy} p_1^4 p_2^2 + d_{xyy} p_1^2 p_2^4, \\ d_x &= C_{11} + C_{55} + C_{66}, \\ d_y &= C_{22} + C_{44} + C_{66}, \\ d_{xx} &= -C_{11}(C_{55}+C_{66}) - C_{55}C_{66}, \\ d_{yy} &= -C_{22}(C_{44}+C_{66}) - C_{44}C_{66}, \\ d_{xy} &= (C_{12}+C_{66})^2 - C_{11}C_{22} - C_{11}C_{44} - C_{22}C_{55} \\ &\quad - (C_{44}+C_{55}+C_{66})C_{66}, \\ d_{xxx} &= C_{11}C_{55}C_{66}, \\ d_{yyy} &= C_{22}C_{44}C_{66}, \\ d_{xxy} &= [C_{11}C_{22} + C_{66}^2 - (C_{12}+C_{66})^2]C_{55} + C_{11}C_{44}C_{66}, \\ d_{xyy} &= [C_{11}C_{22} + C_{66}^2 - (C_{12}+C_{66})^2]C_{44} + C_{22}C_{55}C_{66}. \end{aligned} \quad \text{(B-7)}$$

So far, equations B-3–B-7 are exact and valid for any slowness direction. Our final goal is to derive the effective fourth-order NMO velocity (or anellipticity function), which is an azimuthally dependent coefficient of the traveltime Taylor series expansion for infinitesimal offsets. Considering therefore a near-vertical ray, the vertical-slowness squared may be approximated by the fourth-order expansion (where due to vertical symmetry planes, only even terms are present):

$$p_3^2 = \frac{1}{v_{\text{ver}}^2} - Ap_1^2 - Bp_2^2 + v_{\text{ver}}^2 Cp_1^4 + v_{\text{ver}}^2 Dp_2^4 + v_{\text{ver}}^2 Ep_1^2 p_2^2 + O(p_h^6), \tag{B-8}$$

where $p_h = \sqrt{p_1^2 + p_2^2}$ is the horizontal slowness, and the vertical velocity v_{ver} depends on the wave type:

$$\begin{aligned} &\underbrace{v_{\text{ver}} = \sqrt{C_{33}} = v_P}_{\text{compressional wave}}, \\ &\underbrace{v_{\text{ver}} = v_{S,x_1} = \sqrt{C_{55}} = \sqrt{1-f}\cdot v_P}_{x_1-\text{polarized shear}}, \\ &\underbrace{v_{\text{ver}} = v_{Sx_2} = \sqrt{C_{44}} = \sqrt{1-f}\cdot\frac{\sqrt{1+2\gamma_1}}{\sqrt{1+2\gamma_2}}\cdot v_P}_{x_2-\text{polarized shear}}. \end{aligned} \tag{B-9}$$

A, B, C, D, E are the unknown coefficients, to be established in this appendix. We leave a minus sign before the second-order terms to keep coefficients A and B positive: Normally, an increase in horizontal slowness leads to a decrease in vertical slowness. In particular, for an isotropic medium, $A = B = 1$. Factor v_{ver}^2 applied to the fourth-order terms is used to keep the unknown coefficients normalized (unitless). We introduce the solution form B-8 into the cubic equation B-3, and we ignore all powers or products of order six and higher. For the other terms, we balance the terms with identical powers of p_1 and p_2. This leads to the following results.

P-waves

The second-order coefficients are

$$\begin{aligned} A &= \frac{C_{13}^2 + 2C_{13}C_{55} + C_{33}C_{55}}{C_{33}(C_{33} - C_{55})} = 1 + 2\delta_2, \\ B &= \frac{C_{23}^2 + 2C_{23}C_{44} + C_{33}C_{44}}{C_{33}(C_{33} - C_{44})} = 1 + 2\delta_1. \end{aligned} \tag{B-10}$$

The fourth-order coefficients are

$$C = \frac{1}{C_{33}}\cdot\frac{(C_{13}+C_{55})^4}{(C_{33}-C_{55})^3} - \frac{(C_{13}+C_{55})^2(C_{11}-C_{55})}{C_{33}(C_{33}-C_{55})^2}, \tag{B-11}$$

$$D = \frac{1}{C_{33}}\cdot\frac{(C_{23}+C_{44})^4}{(C_{33}-C_{44})^3} - \frac{(C_{23}+C_{44})^2(C_{22}-C_{44})}{C_{33}(C_{33}-C_{44})^2}, \tag{B-12}$$

$$\begin{aligned} E = {} & \frac{(C_{13}+C_{55})^2(C_{44}-C_{66})}{C_{33}(C_{33}-C_{55})^2} + \frac{(C_{23}+C_{44})^2(C_{55}-C_{66})}{C_{33}(C_{33}-C_{44})^2} \\ & + \frac{(C_{13}+C_{55})^2(C_{23}+C_{44})^2(2C_{33}-C_{44}-C_{55})}{C_{33}(C_{33}-C_{44})^2(C_{33}-C_{55})^2} \\ & - \frac{2(C_{13}+C_{55})(C_{23}+C_{44})(C_{12}+C_{66})}{C_{33}(C_{33}-C_{44})(C_{33}-C_{55})}. \end{aligned} \tag{B-13}$$

Note that for the acoustic approximation, $C_{44} = C_{55} = C_{66} = 0$. According to Alkhalifah (2003), the acoustic approximation accurately describes the kinematics of P-waves. However, in accordance with our computational practice, for relatively strong (but still feasible) anisotropic parameters, the error of the acoustic approximation becomes essential and cannot always be ignored.

S-waves polarized along x_1

The second-order terms are

$$\begin{aligned} A &= \frac{C_{11}}{C_{55}} - \frac{(C_{13}+C_{55})^2}{C_{55}(C_{33}-C_{55})} = 1 + 2\sigma_2, \\ B &= \frac{C_{66}}{C_{55}} = 1 + 2\gamma_1. \end{aligned} \tag{B-14}$$

The fourth-order terms are

$$\begin{aligned} C &= \frac{(C_{11}-C_{55})(C_{13}+C_{55})^2}{(C_{33}-C_{55})^2 C_{55}} - \frac{1}{C_{55}}\cdot\frac{(C_{13}+C_{55})^4}{(C_{33}-C_{55})^3}, \\ D &= 0. \end{aligned} \tag{B-15}$$

$$\begin{aligned} E = {} & -\frac{1}{C_{55}}\cdot\frac{(C_{13}+C_{55})^2(C_{23}+C_{44})^2}{(C_{33}-C_{55})^2(C_{55}-C_{44})} - \frac{(C_{13}+C_{55})^2(C_{44}-C_{66})}{C_{55}(C_{33}-C_{55})^2} \\ & + 2\frac{(C_{13}+C_{55})(C_{23}+C_{44})(C_{12}+C_{66})}{C_{55}(C_{33}-C_{55})(C_{55}-C_{44})} - \frac{1}{C_{55}}\cdot\frac{(C_{12}+C_{66})^2}{C_{55}-C_{44}}. \end{aligned} \tag{B-16}$$

S-waves polarized along the x_2-direction

The second-order terms are

$$\begin{aligned} A &= \frac{C_{66}}{C_{55}} = 1 + 2\gamma_2, \\ B &= \frac{C_{22}}{C_{44}} - \frac{(C_{23}+C_{44})^2}{C_{44}(C_{33}-C_{44})} = 1 + 2\sigma_1\cdot\frac{1+2\gamma_2}{1+2\gamma_1}. \end{aligned} \tag{B-17}$$

The fourth-order terms are

$$\begin{aligned} C &= 0, \\ D &= \frac{(C_{22}-C_{44})(C_{23}+C_{44})^2}{(C_{33}-C_{44})^2 C_{44}} - \frac{1}{C_{44}}\cdot\frac{(C_{23}+C_{44})^4}{(C_{33}-C_{44})^3}. \end{aligned} \tag{B-18}$$

$$\begin{aligned} E = {} & +\frac{1}{C_{44}}\cdot\frac{(C_{13}+C_{55})^2(C_{23}+C_{44})^2}{(C_{33}-C_{44})^2(C_{55}-C_{44})} - \frac{(C_{23}+C_{44})^2(C_{55}-C_{66})}{C_{44}(C_{33}-C_{44})^2} \\ & - 2\frac{(C_{13}+C_{55})(C_{23}+C_{44})(C_{12}+C_{66})}{C_{44}(C_{33}-C_{44})(C_{55}-C_{44})} + \frac{1}{C_{44}}\cdot\frac{(C_{12}+C_{66})^2}{C_{55}-C_{44}}. \end{aligned} \tag{B-19}$$

Parameters σ_1 and σ_2 that appear in equations B-14 and B-17 are dependent and defined as

$$\sigma_1 = \frac{\varepsilon_1 - \delta_1}{1-f}, \quad \sigma_2 = \frac{\varepsilon_2 - \delta_2}{1-f}. \tag{B-20}$$

Note that the fourth-order shear coefficients include items with $C_{55} - C_{44}$ in the denominator. In this paper, we do not consider

S- and converted waves with vertical shear singularity, where $C_{44} = C_{55}$ or $\gamma_1 = \gamma_2$.

We note that further derivations in Appendices C and D are generic and may be related to any pure-mode waves. Derivations in Appendix E may be related to any pure-mode and converted waves.

APPENDIX C

CARTESIAN COMPONENTS OF THE RAY VELOCITY

The ray velocity components may be presented in terms of the slowness surface $p_3(p_1, p_2)$ and its derivatives (Grechka et al., 1997):

$$v_{\text{ray},1} = \frac{-\frac{\partial p_3}{\partial p_1}}{p_3 - \frac{\partial p_3}{\partial p_1} p_1 - \frac{\partial p_3}{\partial p_2} p_2},$$
$$v_{\text{ray},2} = \frac{-\frac{\partial p_3}{\partial p_2}}{p_3 - \frac{\partial p_3}{\partial p_1} p_1 - \frac{\partial p_3}{\partial p_2} p_2},$$
$$v_{\text{ray},3} = \frac{1}{p_3 - \frac{\partial p_3}{\partial p_1} p_1 - \frac{\partial p_3}{\partial p_2} p_2}. \tag{C-1}$$

We assume that the rays are emerging from the reflection point, and therefore, the vertical-slowness is positive. The normalized vertical-slowness $p_3 v_{\text{ver}}$ follows from equation B-8:

$$p_3 v_{\text{ver}} = 1 - \frac{A v_{\text{ver}}^2 p_1^2}{2} - \frac{B v_{\text{ver}}^2 p_2^2}{2} + \frac{4C - A^2}{8} v_{\text{ver}}^4 p_1^4 + \frac{4D - B^2}{8} v_{\text{ver}}^4 p_2^4 + \frac{2E - AB}{4} v_{\text{ver}}^4 p_1^2 p_2^2 + O(p_h^6). \tag{C-2}$$

Substituting equation C-2 into equation C-1 yields the ray velocity components that are listed in equation 10.

APPENDIX D

TRAVELTIME AND OFFSET COMPONENTS VERSUS RAY VELOCITY AND LOCAL EFFECTIVE PARAMETERS

Recall that the radial and transverse components of the offset are defined along and across the slowness azimuth, respectively, and can be added separately through the individual layers. The traveltimes within each layer can also be added. The two-way traveltime Δt_i and two-way offset contributions $\Delta x_{1,i}, \Delta x_{2,i}$ computed in the local frame of the layer are

$$\frac{\Delta x_{1,i}}{\Delta z_i} = 2\frac{v_{\text{ray},1,i}}{v_{\text{ray},3,i}}, \quad \frac{\Delta x_{2,i}}{\Delta z_i} = 2\frac{v_{\text{ray},2,i}}{v_{\text{ray},3,i}}, \quad \frac{\Delta t_i}{\Delta z_i} = \frac{2}{v_{\text{ray},3,i}}, \tag{D-1}$$

where $v_{\text{ray},1,i}, v_{\text{ray},2,i}, v_{\text{ray},3,i}$ are the Cartesian components of the ray velocity computed in the local frame of the ith layer, $\Delta z_i = v_{\text{ver},i}\Delta t_{\text{o},i}/2$ is the layer thickness, and $\Delta t_{\text{o},i}$ is the two-way vertical time. In the radial-transverse frame, the offset components are given by equation 11. The ray velocity components (equation 10) depend on the horizontal-slowness components p_1, p_2 "measured" in the local frame. It is suitable to express them through the magnitude p_h and azimuth ψ_{slw} of the horizontal slowness (which are constant through all layers):

$$p_1 = p_h \cos(\psi_{\text{slw}} - \psi_{x_1,i}), \quad p_2 = p_h \sin(\psi_{\text{slw}} - \psi_{x_1,i}). \tag{D-2}$$

The slowness azimuth ψ_{slw} is measured in the global frame. Substituting equation D-2 into equation 10 and continuous insertion of the resulting equation into equation 11 results in equation 12, which includes three local effective second-order parameters $u_{2,i}, w_{2x,i}, w_{2y,i}$ and five local effective fourth-order parameters $u_{4,i}, w_{42x,i}, w_{42y,i}, w_{44x,i}, w_{44y,i}$. For a single orthorhombic layer, due to its vertical symmetry planes, only three local effective fourth-order parameters are independent. However, the global effective parameters are all independent.

The global effective model yields the same traveltime and offset components as the original layered model, within the prescribed accuracy. The local effective parameters in the series expansion for the radial and transverse offset components and the traveltime delivered by equation 12 depend on the five coefficients A, B, C, D, E of the vertical-slowness surface obtained in Appendix B. The second-order parameters are

$$u_{2,i} = \frac{A_i + B_i}{2} v_{\text{ver},i}^2 \Delta t_{\text{o},i},$$
$$w_{2x,i} = \frac{A_i - B_i}{2} \cos 2\psi_{x_1,i} v_{\text{ver},i}^2 \Delta t_{\text{o},i},$$
$$w_{2y,i} = \frac{A_i - B_i}{2} \sin 2\psi_{x_1,i} v_{\text{ver},i}^2 \Delta t_{\text{o},i}. \tag{D-3}$$

The fourth-order parameters are

$$u_{4,i} = \left(\frac{3A_i^2 + 2A_iB_i + 3B_i^2}{16} - \frac{3C_i + 3D_i + E_i}{4}\right) v_{\text{ver},i}^4 \Delta t_{\text{o},i},$$
$$w_{42x,i} = \left(\frac{A_i^2 - B_i^2}{4} - C_i + D_i\right) v_{\text{ver},i}^4 \Delta t_{\text{o},i} \cos 2\psi_{x_1,i},$$
$$w_{42y,i} = \left(\frac{A_i^2 - B_i^2}{4} - C_i + D_i\right) v_{\text{ver},i}^4 \Delta t_{\text{o},i} \sin 2\psi_{x_1,i},$$
$$w_{44x,i} = \left[\frac{(A_i - B_i)^2}{16} - \frac{C_i + D_i - E_i}{4}\right] v_{\text{ver},i}^4 \Delta t_{\text{o},i} \cos 4\psi_{x_1,i},$$
$$w_{44y,i} = \left[\frac{(A_i - B_i)^2}{16} - \frac{C_i + D_i - E_i}{4}\right] v_{\text{ver},i}^4 \Delta t_{\text{o},i} \sin 4\psi_{x_1,i}. \tag{D-4}$$

Vertically varying parameters within the layers

Our method makes it possible to compute the local and global effective parameters of layered models characterized with vertically varying piecewise-continuous parameters, and discontinuities at the interfaces between the layers. In this case, equations D-3 and D-4 represent differential increments, to be integrated. All parameters in the equations become instantaneous parameters versus vertical time or depth. The first equation D-3 for piecewise-continuous model reads

$$du_{2,i} = \frac{A_i(\tau) + B_i(\tau)}{2} v^2_{\mathrm{ver},i}(\tau) d\tau, \tag{D-5}$$

where τ is the running vertical time. Integration over the layer thickness or two-way vertical time leads to

$$\begin{aligned} u_{2,i} &= \int_{t_{\mathrm{o},i}}^{t_{\mathrm{o},i}+\Delta t_{\mathrm{o},i}} \frac{A_i(\tau) + B_i(\tau)}{2} v^2_{\mathrm{ver},i}(\tau) d\tau \\ &= 2 \int_{z_i}^{z_i+\Delta z_i} \frac{A_i(z) + B_i(z)}{2} v_{\mathrm{ver},i}(z) dz, \end{aligned} \tag{D-6}$$

where $t_{\mathrm{o},i}$ and z_i are the two-way vertical time and depth of the upper interface of the layer (vertical time and depth are increasing downward). A practical particular case is a layer whose vertical compressional velocity varies continuously with depth (or vertical time), but the other parameters (shear parameter f, Tsvankin's orthorhombic parameters, and azimuths of the vertical symmetry planes) are constant through the layer. Recall that the vertical slowness coefficients $A_i, \ldots, E_i$ are normalized (unitless) ratios of the stiffness matrix coefficients, and in case only the vertical compressional velocity changes, all stiffness components change in a proportional manner, so that the slowness coefficients $A_i, \ldots, E_i$ remain unchanged. In this case, equation D-6 simplifies to

$$\begin{aligned} u_{2,i} &= \frac{A_i + B_i}{2} \int_{t_{\mathrm{o},i}}^{t_{\mathrm{o},i}+\Delta t_{\mathrm{o},i}} v^2_{\mathrm{ver},i}(\tau) d\tau \\ &= (A_i + B_i) \int_{z_i}^{z_i+\Delta z_i} v_{\mathrm{ver},i}(z) dz. \end{aligned} \tag{D-7}$$

Other equations of sets D-3 and D-4 have to be converted accordingly, which means that the powers of vertical velocity $v^2_{\mathrm{ver},i}$ and $v^4_{\mathrm{ver},i}$ have to be replaced by the powers of local rms and local root-mean-quad (rmq) of the vertical velocity, $v^2_{\mathrm{rms},i}$ and $v^4_{\mathrm{rmq},i}$; accordingly,

$$\begin{aligned} v^2_{\mathrm{rms},i} &= \frac{1}{\Delta t_{\mathrm{o},i}} \int_{t_{\mathrm{o},i}}^{t_{\mathrm{o},i}+\Delta t_{\mathrm{o},i}} v^2_{\mathrm{ver},i}(\tau) d\tau, \\ v^4_{\mathrm{rmq},i} &= \frac{1}{\Delta t_{\mathrm{o},i}} \int_{t_{\mathrm{o},i}}^{t_{\mathrm{o},i}+\Delta t_{\mathrm{o},i}} v^4_{\mathrm{ver},i}(\tau) d\tau. \end{aligned} \tag{D-8}$$

The two-way vertical time $\Delta t_{\mathrm{o},i}$ is related to the layer thickness:

$$\Delta t_{\mathrm{o},i} = \int_{z_i}^{z_i+\Delta z_i} \frac{2dz}{v_{\mathrm{ver},i}(z)} = \frac{2\Delta z_i}{v_{\mathrm{ave},i}}, \tag{D-9}$$

where $v_{\mathrm{ave},i}$ is the interval (local average) velocity of the given layer. Note that the vertical velocities depend on the wave type.

For pure mode waves, parameter $\Delta t_{\mathrm{o},i}$ is the two-way vertical time, and for converted waves, $\Delta t_{\mathrm{o},i}$ is the one-way vertical time. To obtain the global effective parameters for converted waves, we compute and stack the local effective parameters twice: first for the incident wave and then for reflected.

APPENDIX E

FOURTH-ORDER NMO VELOCITY IN THE SLOWNESS-AZIMUTH/OFFSET DOMAIN

The eight global effective parameters yield the desired fourth-order NMO velocity for any slowness azimuth. It can be presented as a product of a second-order normalizing factor $K_{2,\mathrm{off}}(\psi_{\mathrm{slw}})$ and a fourth-order kernel $K_{4,\mathrm{off}}(\psi_{\mathrm{slw}})$, as shown in equation 26. The normalizing factor reads

$$\begin{aligned} &K_{2,\mathrm{off}}(\psi_{\mathrm{slw}}) \\ &= t_{\mathrm{o}}^{-1} \cdot \frac{U_2^2 + W_{2x}^2 + W_{2y}^2 + 2U_2 W_{2x} \cos 2\psi_{\mathrm{phs}} + 2U_2 W_{2y} \sin 2\psi_{\mathrm{slw}}}{(U_2 + W_{2x} \cos 2\psi_{\mathrm{slw}} + W_{2y} \sin 2\psi_{\mathrm{slw}})^4} \\ &= t_{\mathrm{o}}^{-1} \cdot \frac{U_2^2 + W_2^2 + 2U_2 W_2 \cos 2(\psi_{\mathrm{slw}} - \Psi_{2,\mathrm{H}})}{[U_2 + W_2 \cos 2(\psi_{\mathrm{slw}} - \Psi_{2,\mathrm{H}})]^4} \end{aligned} \tag{E-1}$$

or alternatively,

$$\begin{aligned} &K_{2,\mathrm{off}}(\psi_{\mathrm{slw}}) \\ &= t_{\mathrm{o}}^{-3} \cdot \frac{V_{2,\mathrm{H}}^4 \cos^2(\psi_{\mathrm{slw}} - \Psi_{2,\mathrm{H}}) + V_{2,\mathrm{L}}^4 \sin^2(\psi_{\mathrm{slw}} - \Psi_{2,\mathrm{H}})}{[V_{2,\mathrm{H}}^2 \cos^2(\psi_{\mathrm{slw}} - \Psi_{2,\mathrm{H}}) + V_{2,\mathrm{L}}^2 \sin^2(\psi_{\mathrm{slw}} - \Psi_{2,\mathrm{H}})]^4}. \end{aligned} \tag{E-2}$$

The normalizing factor $K_{2,\mathrm{off}}(\psi_{\mathrm{slw}})$ includes only the second-order parameters, $U_2, W_2, \Psi_{2,\mathrm{H}}$, or equivalently the high and low global second-order NMO velocities and the azimuth of the global high second-order NMO velocity, $V_{2,\mathrm{L}}, V_{2,\mathrm{H}}, \Psi_{2,\mathrm{H}}$. The kernel $K_{4,\mathrm{off}}(\psi_{\mathrm{slw}})$ of the global fourth-order NMO velocity may be presented in a bilinear form:

$$K_{4,\mathrm{off}}(\psi_{\mathrm{slw}}) = \mathbf{m}\mathbf{M}_{\mathrm{slw/off}}\mathbf{a}_{\mathrm{slw},7}, \tag{E-3}$$

where $\mathbf{m}$ is a row vector of length 5 that includes global effective fourth-order parameters,

$$\mathbf{m} = [\, U_4 \quad W_{42x} \quad W_{42y} \quad W_{44x} \quad W_{44y} \,], \tag{E-4}$$

$\mathbf{a}_{\mathrm{slw},7}$ is a column vector of length 7 that depends on the slowness azimuth alone,

$$\begin{aligned} \mathbf{a}_{\mathrm{slw},7} = [&1, \cos 2\psi_{\mathrm{slw}}, \sin 2\psi_{\mathrm{slw}}, \cos 4\psi_{\mathrm{slw}}, \sin 4\psi_{\mathrm{slw}}, \\ &\cos 6\psi_{\mathrm{slw}}, \sin 6\psi_{\mathrm{slw}}]^{\mathrm{T}}, \end{aligned} \tag{E-5}$$

and $\mathbf{M}_{\mathrm{slw/off}}$ is a matrix of dimension 5×7, whose components depend on the second-order parameters. Column 1,

$$\begin{aligned} M_{\mathrm{slw/off},11} &= +2(U_2^2 - W_{2x}^2 - W_{2y}^2) \\ M_{\mathrm{slw/off},21} &= +4U_2 W_{2x} \\ M_{\mathrm{slw/off},31} &= +4U_2 W_{2y} \\ M_{\mathrm{slw/off},41} &= +4(W_{2x}^2 - W_{2y}^2) \\ M_{\mathrm{slw/off},51} &= +8W_{2x} W_{2y} \end{aligned} \quad ; \tag{E-6}$$

columns 2 and 3,

$$\begin{array}{ll} M_{\mathrm{slw/off},12} = +4U_2W_{2x} & M_{\mathrm{slw/off},13} = +4U_2W_{2y} \\ M_{\mathrm{slw/off},22} = +2U_2^2 + W_{2x}^2 - 5W_{2y}^2 & M_{\mathrm{slw/off},23} = +6W_{2x}W_{2y} \\ M_{\mathrm{slw/off},32} = +6W_{2x}W_{2y} & M_{\mathrm{slw/off},33} = +2U_2^2 - 5W_{2x}^2 + W_{2y}^2 ; \\ M_{\mathrm{slw/off},42} = +6U_2W_{2x} & M_{\mathrm{slw/off},43} = -6U_2W_{2y} \\ M_{\mathrm{slw/off},52} = +6U_2W_{2y} & M_{\mathrm{slw/off},53} = +6U_2W_{2x} \end{array} \tag{E-7}$$

columns 4 and 5,

$$\begin{array}{ll} M_{\mathrm{slw/off},14} = 4(W_{2x}^2 - W_{2y}^2) & M_{\mathrm{slw/off},15} = 8W_{2x}W_{2y} \\ M_{\mathrm{slw/off},24} = 0 & M_{\mathrm{slw/off},25} = 0 \\ M_{\mathrm{slw/off},34} = 0 & M_{\mathrm{slw/off},35} = 0 \quad ; \\ M_{\mathrm{slw/off},44} = 2(U_2^2 - W_{2x}^2 - W_{2y}^2) & M_{\mathrm{slw/off},45} = 0 \\ M_{\mathrm{slw/off},54} = 0 & M_{\mathrm{slw/off},55} = 2(U_2^2 - W_{2x}^2 - W_{2y}^2) \end{array} \tag{E-8}$$

and columns 6 and 7,

$$\begin{array}{ll} M_{\mathrm{slw/off},16} = 0 & M_{\mathrm{slw/off},17} = 0 \\ M_{\mathrm{slw/off},26} = +W_{2x}^2 - W_{2y}^2 & M_{\mathrm{slw/off},27} = +2W_{2x}W_{2y} \\ M_{\mathrm{slw/off},36} = -2W_{2x}W_{2y} & M_{\mathrm{slw/off},37} = +W_{2x}^2 - W_{2y}^2 . \\ M_{\mathrm{slw/off},46} = -2U_2W_{2x} & M_{\mathrm{slw/off},47} = -2U_2W_{2y} \\ M_{\mathrm{slw/off},56} = +2U_2W_{2y} & M_{\mathrm{slw/off},57} = -2U_2W_{2x} \end{array} \tag{E-9}$$

LIST OF SYMBOLS

Interval parameters

v_P	=	vertical compressional velocity of the orthorhombic layer
v_{S,x_1}, v_{S,x_2}	=	vertical velocities of S-waves, polarized in the x_1 and x_2 directions
v_{Pb}, v_{Sb}	=	vertical compressional and shear velocities of the background VTI layer (VFTI)
$f = \frac{v_P^2 - v_{S,x_1}^2}{v_P^2}$	=	coefficient depending on the ratio between vertical shear velocity, polarized in the x_1 direction, and the vertical compressional velocity
$f_b = \frac{v_{Pb}^2 - v_{Sb}^2}{v_{Pb}^2}$	=	coefficient depending on the ratio between the vertical shear and vertical compressional velocities, for VTI background layer (VFTI)
$\delta, \varepsilon, \gamma$	=	Thomsen parameters of VTI background media
$\delta_1, \delta_2, \delta_3, \varepsilon_1, \varepsilon_2, \gamma_1, \gamma_2$	=	Tsvankin's (1997) orthorhombic parameters
$\Delta_{\mathrm{n}_i}, \Delta_{\mathrm{v}_i}, \Delta_{\mathrm{h}_i}$	=	normal, vertical tangential, and horizontal tangential weakness; $i = 1, 2$ is the index of horizontal axis, normal to the fracture plane
Δz_i	=	layer thickness
C_{ij}	=	density-normalized components of the stiffness matrix, $i, j = 1, \ldots, 6$
Γ_{ik}	=	components of the Christoffel matrix; $i, k = 1, 2, 3$
A, B, C, D, E	=	fourth-order series coefficients of the vertical-slowness series
$\Delta h_{R,i}$	=	local radial-offset component
$\Delta h_{T,i}$	=	local transverse-offset component
$\Delta x_{k,i}$	=	contribution of the ith layer of the total offset components in the global frame, $k = 1, 2$
Δt_i	=	local traveltime (two way if not specified)
$\Delta t_{\mathrm{o},i}$	=	local vertical time (two way if not specified)
v_{phs}	=	magnitude of the phase velocity
v_{ver}	=	local vertical velocity (for a specific wave type)
v_{ave}	=	interval (local average) velocity
v_{rms}	=	local rms velocity
v_{rmq}	=	local rmq velocity
$v_{\mathrm{ray},i}$	=	Cartesian components of the ray velocity in the local frame, $i = 1, 2, 3$
$u_{2,i}, w_{2x,i}, w_{2y,i}$	=	local second-order effective parameters
$u_{4,i}, w_{42x,i}, w_{42y,i}, w_{44x,i}, w_{44y,i}$	=	local fourth-order effective parameters

Global parameters

p_h	=	magnitude of horizontal-slowness vector
p_1, p_2, p_3	=	slowness vector components (p_3 is not a global parameter)
h_R	=	radial-offset component
h_T	=	transverse-offset component
h	=	offset
$\bar{h}$	=	normalized offset
t_{o}	=	two-way vertical time
t	=	two-way traveltime
$\bar{t}$	=	normalized two-way traveltime
z	=	depth of the reflector point
xyz	=	global frame of reference
$V_{2,\mathrm{L}}$	=	global low second-order NMO velocity
$V_{2,\mathrm{H}}$	=	global high second-order NMO velocity
α	=	normalized asymptotic correction factor of the traveltime approximation
$V_2(\psi)$	=	generic azimuthally dependent global second-order NMO velocity
$V_4(\psi)$	=	generic azimuthally dependent global fourth-order NMO velocity
$V_{2,\mathrm{slw}}(\psi_{\mathrm{slw}})$	=	slowness-azimuth/slowness domain global second-order NMO velocity
$V_{4,\mathrm{slw}}(\psi_{\mathrm{slw}})$	=	slowness-azimuth/slowness domain global fourth-order NMO velocity
$V_{2,\mathrm{off}}(\psi_{\mathrm{slw}})$	=	slowness-azimuth/offset domain global second-order NMO velocity
$V_{4,\mathrm{off}}(\psi_{\mathrm{slw}})$	=	slowness-azimuth/offset domain global fourth-order NMO velocity
$V_{2,\mathrm{slw}}(\psi_{\mathrm{off}})$	=	offset-azimuth/slowness domain global second-order NMO velocity
$V_{4,\mathrm{slw}}(\psi_{\mathrm{off}})$	=	offset-azimuth/slowness domain global fourth-order NMO velocity

$V_{2,\mathrm{off}}(\psi_{\mathrm{off}})$ = offset-azimuth/offset domain global second-order NMO velocity

$V_{4,\mathrm{off}}(\psi_{\mathrm{off}})$ = offset-azimuth/offset domain global fourth-order NMO velocity

$K_{2,\mathrm{off}}(\psi_{\mathrm{slw}})$ = slowness-azimuth/offset domain normalizing factor of fourth-order NMO velocity

$K_{4,\mathrm{off}}(\psi_{\mathrm{slw}})$ = slowness-azimuth/offset domain kernel of fourth-order NMO velocity

$\mathbf{m}$ = row vector of length 5 containing global fourth-order effective parameters

$\mathbf{M}_{\mathrm{slw/off}}$ = matrix of dimensions 5×7; it depends on second-order effective parameters, needed to compute fourth-order NMO velocity, in the slowness-azimuth/offset domain

$\mathbf{a}_{\mathrm{slw},7}$ = vector of length 7; it depends on slowness-azimuth only

$\eta_{\mathrm{eff}}(\psi)$ = azimuthally dependent global effective anellipticity in slowness-azimuth or offset-azimuth domains

$A_4(\psi)$ = quartic coefficient related to moveout anellipticity in the slowness-azimuth or offset-azimuth domains

U_2, W_{2x}, W_{2y} = global effective second-order parameters

$U_4, W_{42x}, W_{42y}, W_{44x}, W_{44y}$ = global effective fourth-order parameters

Local zenith angles for layer i

$\theta_{\mathrm{slw},i}$ = slowness (phase) angle between the slowness direction and the vertical axis

$\theta_{\mathrm{slw,H}}$ = slowness (phase) angle of the high-velocity layer, angle between slowness direction for that layer and vertical axis

$\theta_{\mathrm{ray},i}$ = ray angle between the ray (group) velocity direction and the vertical axis

$\theta_{\mathrm{ray,H}}$ = ray angle of the high-velocity layer, angle between the ray velocity direction for that layer and the vertical axis

Local and global azimuths

ψ_{x_1} = azimuth of local orthorhombic axis x_1

$\psi_{\mathrm{ray},i}$ = local ray (group) velocity azimuth within layer i

ψ_{slw} = slowness azimuth (also, azimuth of horizontal slowness or phase velocity)

ψ_{off} = offset azimuth (azimuth of acquisition source-receiver offsets)

ψ = general azimuth; it may be either slowness azimuth or offset azimuth

$\Psi_{2,\mathrm{L}}$ = azimuth of global low second-order NMO velocity

$\Psi_{2,\mathrm{H}}$ = azimuth of global high second-order NMO velocity

REFERENCES

Al-Dajani, A., and N. Toksoz, 2001, Non-hyperbolic reflection moveout for orthorhombic media: Technical Report, Earth Resources Laboratory Industry Consortia Annual Report, 2002–07.

Al-Dajani, A., and I. Tsvankin, 1998, Non-hyperbolic reflection moveout for horizontal transverse isotropy: Geophysics, **63**, 1738–1753, doi: 10.1190/1.1444469.

Al-Dajani, A., I. Tsvankin, and N. Toksoz, 1998, Non-hyperbolic reflection moveout for azimuthally anisotropic media: 68th Annual International Meeting, SEG, Expanded Abstracts, 1479–1482.

Alkhalifah, T., 1997, Velocity analysis using nonhyperbolic moveout in transversely isotropic media: Geophysics, **62**, 1839–1854, doi: 10.1190/1.1444285.

Alkhalifah, T., 2003, An acoustic wave equation for orthorhombic anisotropy: Geophysics, **68**, 1169–1172, doi: 10.1190/1.1598109.

Alkhalifah, T., and I. Tsvankin, 1995, Velocity analysis for transversely isotropic media: Geophysics, **60**, 1550–1566, doi: 10.1190/1.1443888.

Bakulin, A., V. Grechka, and I. Tsvankin, 2000, Estimation of fracture parameters from reflection seismic data — Part 2: Fractured models with orthorhombic symmetry: Geophysics, **65**, 1803–1817, doi: 10.1190/1.1444864.

Bakulin, A., V. Grechka, and I. Tsvankin, 2002, Seismic inversion for the parameters of two orthogonal fracture sets in a VTI background medium: Geophysics, **67**, 292–299, doi: 10.1190/1.1451801.

Červený, V., 2001, Seismic ray theory: Cambridge University Press.

Dix, C., 1955, Seismic velocities from surface measurements: Geophysics, **20**, 68–86, doi: 10.1190/1.1438126.

Eshelby, J., 1957, The determination of the elastic field of an ellipsoidal inclusion and related problems: Proceedings of the Royal Society of London, **A241**, 376–396, doi: 10.1098/rspa.1957.0133.

Gerea, C., L. Nicoletis, and P. Granger, 2000, Multicomponent true-amplitude anisotropic imaging — "Fractures, converted waves and case studies": Proceedings of the 9th IWSA International Workshop on Seismic Anisotropy, Expanded Abstracts, doi: 10.1190/1.9781560801771.

Grechka, V., 2007, Multiple cracks in VTI rocks: Effective properties and fracture characterization: Geophysics, **72**, no. 5, D81–D91, doi: 10.1190/1.2751500.

Grechka, V., and I. Tsvankin, 1998, 3-D description of normal moveout in anisotropic inhomogeneous media: Geophysics, **63**, 1079–1092, doi: 10.1190/1.1444386.

Grechka, V., and I. Tsvankin, 1999, 3-D moveout velocity analysis and parameter estimation for orthorhombic media: Geophysics, **64**, 820–837, doi: 10.1190/1.1444593.

Grechka, V., I. Tsvankin, and J. Cohen, 1997, Generalized Dix equation and analytic treatment of normal-moveout velocity for anisotropic media: 67th Annual International Meeting, SEG, Expanded Abstracts, 1246–1249.

Hao, Q., and A. Stovas, 2015, Anelliptic approximation for P-wave phase and group velocities in orthorhombic media: 77th Annual International Conference and Exhibition, EAGE, Extended Abstracts, doi: 10.3997/2214-4609.201413004.

Hao, Q., and A. Stovas, 2016, Analytic calculation of phase and group velocities of P-wave in orthorhombic media: Geophysics, **81**, no. 3, C79–C97, doi: 10.1190/geo2015-0156.1.

Helbig, K., and M. Schoenberg, 1987, Anomalous polarization of elastic waves in transversely isotropic media: Journal of the Acoustical Society of America, **81**, 1235–1245, doi: 10.1121/1.394527.

Ivanov, Y., and A. Stovas, 2016, S-waves normal moveout velocity ellipse in vicinity of the singularity point in tilted ORT media:17th International Workshop on Seismic Anisotropy, Extended Abstracts, 3–4.

Koren, Z., and I. Ravve, 2011, Full-azimuth subsurface angle domain wavefield decomposition and imaging — Part 1: Directional and reflection image gathers: Geophysics, **76**, no. 1, S1–S13, doi: 10.1190/1.3511352.

Koren, Z., and I. Ravve, 2014, Azimuthally-dependent anisotropic velocity model update: Geophysics, **79**, no. 2, C27–C53, doi: 10.1190/geo2013-0178.1.

Koren, Z., and I. Ravve, 2015, Fourth-order NMO velocity for compressional waves in layered orthorhombic medium: 77th Annual International Conference and Exhibition, EAGE, Extended Abstracts, doi: 10.3997/2214-4609.201412573.

Koren, Z., and I. Ravve, 2016, Fourth-order NMO velocity for P-waves in layered orthorhombic media vs. offset azimuth: 86th Annual International Meeting, SEG, Expanded Abstracts, 436–440.

Koren, Z., I. Ravve, and R. Levy, 2010, Moveout approximation for horizontal transversely isotropic and vertical transversely isotropic layered medium — Part 2: Effective model: Geophysical Prospecting, **58**, 599–617, doi: 10.1111/j.1365-2478.2009.00857.x.

Koren, Z., I. Ravve, and R. Levy, 2013, Conversion of background VTI depth model and full-azimuth reflection angle moveouts into interval orthorhombic layered parameters: 75th Annual International Conference and Exhibition, EAGE, Extended Abstracts, doi: 10.3997/2214-4609.20130943.

Pech, A., I. Tsvankin, and V. Grechka, 2003, Quartic moveout coefficient: 3D description and application to tilted TI media: Geophysics, **68**, 1600–1610, doi: 10.1190/1.1620634.

Pech, A., and I. Tsvankin, 2004, Quartic moveout coefficient for a dipping azimuthally anisotropic layer: Geophysics, **69**, 699–707, doi: 10.1190/1.1759456.

Ravve, I., and Z. Koren, 2010, Moveout approximation for horizontal transversely isotropic and vertical transversely isotropic layered medium — Part 1: 1D ray propagation: Geophysical Prospecting, **58**, 577–597, doi: 10.1111/j.1365-2478.2009.00856.x.

Ravve, I., and Z. Koren, 2011, Full-azimuth subsurface angle domain wavefield decomposition and imaging — Part 2: Local angle domain: Geophysics, **76**, no. 2, S51–S64, doi: 10.1190/1.3549742.

Ravve, I., and Z. Koren, 2013, Moveout approximation for compressional waves in layered orthorhombic medium: 75th Annual International Conference and Exhibition, EAGE, Extended Abstracts, doi: 10.3997/2214-4609.20130022.

Ravve, I., and Z. Koren, 2015a, Normal moveout velocity for pure-mode and converted waves in layered orthorhombic medium: Geophysical Prospecting, **64**, 1235–1258, doi: 10.1111/1365-2478.12340.

Ravve, I., and Z. Koren, 2015b, Long-offset asymptotic moveout for compressional waves in layered orthorhombic medium: 77th Annual International Conference and Exhibition, EAGE, Extended Abstracts, doi: 10.3997/2214-4609.201413045.

Ravve, I., and Z. Koren, 2016, Fourth-order NMO velocity for P-waves in layered orthorhombic media vs. phase azimuth: 86th Annual International Meeting, SEG, Expanded Abstracts, 469–473.

Schoenberg, M., and J. Douma, 1988, Elastic wave propagation in media with parallel fractures and aligned cracks: Geophysical Prospecting, **36**, 571–590, doi: 10.1111/j.1365-2478.1988.tb02181.x.

Schoenberg, M., and K. Helbig, 1997, Orthorhombic media: Modeling elastic wave behavior in a vertically fractured earth: Geophysics, **62**, 1954–1974, doi: 10.1190/1.1444297.

Sripanich, Y., and S. Fomel, 2014, Anelliptic approximations for qP velocities in orthorhombic media: 84th Annual International Meeting, SEG, Expanded Abstracts, 409–414.

Sripanich, Y., and S. Fomel, 2016, Theory of interval traveltime parameter estimation in layered anisotropic media: Geophysics, **81**, no. 5, C253–C263, doi: 10.1190/geo2016-0013.1.

Stovas, A., 2015, Azimuthally-dependent kinematic properties of orthorhombic media: Geophysics, **80**, no. 6, C107–C122, doi: 10.1190/geo2015-0288.1.

Thomsen, L., 1986, Weak elastic anisotropy: Geophysics, **51**, 1954–1966, doi: 10.1190/1.1442051.

Tsvankin, I., 1997, Anisotropic parameters and P-wave velocity for orthorhombic media: Geophysics, **62**, 1292–1309, doi: 10.1190/1.1444231.

Tsvankin, I., and L. Thomsen, 1994, Nonhyperbolic reflection moveout in anisotropic media: Geophysics, **59**, 1290–1304, doi: 10.1190/1.1443686.

Vasconcelos, I., and I. Tsvankin, 2006, Non-hyperbolic moveout inversion of wide-azimuth P-wave data for orthorhombic media: Geophysical Prospecting, **54**, 535–552, doi: 10.1111/j.1365-2478.2006.00559.x.

Xu, X., I. Tsvankin, and A. Pech, 2005, Geometrical spreading of P-waves in horizontally layered, azimuthally anisotropic media: Geophysics, **70**, no. 5, D43–D53, doi: 10.1190/1.2052467.